Land Use Policy 157 (2025) 107680

Contents lists available at ScienceDirect

Land Use Policy

journal homepage: www.elsevier.com/locate/landusepol

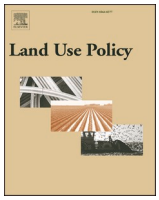

Traceability and projected patterns of Africa's land use systems and climate variability (1993–2053)

Emmanuel Yeboah [a], Isaac Sarfo [b,i], Qiankun Zhu [b,j,*], Clement Kwang [c], Dzifa Adimle Puplampu [d], Ebenezer Nikoi [c], Isaac K. Arthur [c], Alex Barimah Owusu [c], Iris Ekua Mensimah Fynn [c], Charafa El Rhadiouini [a], Abraham Okrah [e], Ali Hasan Jaffry [a], Fareeha Siddique [a], Rukhshinda Aftab [a], Dinah Boyetey [f], Williams Siaw [g], Sabastian Batasuma [h]

[a] School of Remote Sensing and Geomatics Engineering, Nanjing University of Information Science and Technology, Nanjing, Jiangsu 210044, China
[b] College of Geography and Environmental Science, Henan University, Kaifeng, Henan Province 475004, China
[c] Department of Geography and Resource Development, University of Ghana, Legon-Accra, Ghana
[d] School of Environmental Sciences, University of Hull, Hull, United Kingdom
[e] Collaborative Innovation Center on Forecast and Evaluation of Meteorological Disaster, Nanjing University of Information Science and Technology, Nanjing, Jiangsu 210044, China
[f] School of Business, Nanjing University of Information Science and Technology, Nanjing, Jiangsu 210044, China
[g] Department of Management Science Engineering, Nanjing University of Information Science and Technology, Nanjing, Jiangsu 210044, China
[h] College of Economics and management, Taiyuan university of Technology, Taiyuan city, Shanxi Province, China
[i] Organization of African Academic Doctors (OAAD), Off Kamiti Road, Nairobi P.O. Box 25305000100, Kenya
[j] Key Laboratory of Geospatial Technology for the Middle and Lower Yellow River Regions (Henan University), Ministry of Education, Kaifeng, 475004 China

ARTICLE INFO

Keywords:
Land Use and Land Cover Change
Temperature
Precipitation
Geographical Convergence Cross Mapping
Convergence Cross Mapping
Africa

ABSTRACT

This study investigates the causality between land use and land cover change (LULCC), and variations in temperature and precipitation across Africa. To do this, we employ integrated remote sensing techniques, causal analyses, and representative studies. We further utilize Modules for Land Use Change Evaluation (MOLUSCE) and Random Forest (RF) to simulate land use scenarios from 2033 to 2053. The findings reveal a complex interplay of socio-political, economic, and biophysical factors driving LULCC from 1993 to 2023. During this period, northern and western Africa experienced forest regrowth (+2.61 %), while deserts (-12.29 %), grassland/shrubs (-14.20 %), and farmlands (-14.53 %) decreased. In contrast, built-up areas expanded by + 134.63 %, and water bodies increased by + 71.63 %. The predicted trends indicate continued reductions in deserts and bare land, with annual decreases of 0.59 % and a decline of 0.48 % for grasslands/shrubs over the next 30 years. The current study achieved a 96 % accuracy rate based on the samples used throughout the study duration. Rising temperatures in northern Africa are associated with increased desertification, while dense forests and water bodies in central and southern Africa help mitigate heat. K-means clustering identifies distinct regional patterns in the impacts of LULCC, stressing the need for targeted interventions. The insights generated will be valuable for regions with limited resources and institutional capacity to address environmental challenges associated with these undesired changes. Ultimately, these findings can foster stronger collaboration within Africa's economic blocs, supporting regional efforts toward sustainable development, effective land management, and climate adaptation.

* Corresponding author at: College of Geography and Environmental Science, Henan University, Kaifeng, Henan Province 475004, China.
E-mail addresses: emmanuelyeboah@nuist.edu.cn (E. Yeboah), isaacsarfo@henu.edu.cn (I. Sarfo), Zhuqk@henu.edu.cn (Q. Zhu), ckwang@ug.edu.gh (C. Kwang), sayahjifa@gmail.com (D.A. Puplampu), enikoi@ug.edu.gh (E. Nikoi), ikarthur@ug.edu.gh (I.K. Arthur), abowusu@ug.edu.gh (A.B. Owusu), iemfynn@ug.edu.gh (I.E.M. Fynn), charafa.elrhadiouini@gmail.com (C. El Rhadiouini), okrahabraham2014@gmail.com (A. Okrah), alijafrey1122@gmail.com (A.H. Jaffry), fareehasiddique01@gmail.com (F. Siddique), rukhshinda.aftab@gmail.com (R. Aftab), dinahboyetey@nuist.edu.cn (D. Boyetey), 202352250006@nuist.edu.cn (W. Siaw), zsabastian7@gmail.com (S. Batasuma).

https://doi.org/10.1016/j.landusepol.2025.107680
Received 15 November 2024; Received in revised form 15 May 2025; Accepted 25 June 2025
Available online 3 July 2025
0264-8377/© 2025 Elsevier Ltd. All rights are reserved, including those for text and data mining, AI training, and similar technologies.

1. Introduction

As Africa continues to experience rapid population growth, it is expected that by the year 2100, two out of every five individuals on earth are expected to be African (UN-Habitat, 2022). This will translate into Africa holding the largest population percentage of 40 % (4.2 billion) globally. Before 2100, Africa is expected to hold 25 % (2.5 billion) of the world's population in 2050. Presently, Africa holds the second highest population percentage of 18.15 % (1.4 billion) across the globe from 9 % in 1900 (140 million). The fast-paced growth rate of Africa informed by a youthful population, high fertility rates and low mortality rates commands attention as its demographic transformation will transform/shape both the urban and peripheral landscapes as the demand for infrastructure, food, water and energy escalates (Pieterse and Parnell, 2014). This transformation will not only affect the African continent but will reverberate globally.

Presently, demographic factors such as rapid population growth and rural-to-urban migration have collectively influenced land use trends, resulting in urban expansion and the conversion of agricultural land into built-up areas in many African countries. For instance, cities like Lagos (Nigeria) and Nairobi (Kenya) are experiencing rapid urbanization due to population pressures, which have been projected to worsen livelihoods in Africa (Moore et al., 2015). Social factors such as changing lifestyles and cultural land ownership systems are also contributing to land use changes, with younger generations moving away from traditional agricultural practices toward urban employment. Additionally, economic factors like economic growth, foreign direct investment, and the shift toward large-scale commercial agriculture have increased the demand for land, driving deforestation and the expansion of urban areas. In countries like Ghana and Ethiopia, agricultural land and forests are being converted into residential and commercial spaces, achieving some economic benefits and increasing GDP. Political factors play a key role as well, with government policies in North African countries like Morocco and Algeria focusing on afforestation strategies to cushion livelihoods and combat environmental degradation, while countries in West and East Africa, such as Kenya and Ghana, face policy-driven urbanization and infrastructure development that accelerate land use conversion. These trends reflect complex interactions between demographic, social, economic, and political forces that are shaping land use patterns across the continent, with both positive and negative impacts on local communities and ecosystems (Sarfo et al., 2024; Oduro et al., 2025). Nonetheless, these benefits are stifled by environmental and social implications that are emerging as a result of land use changes associated with the transformation of land covers. Specifically, these trends have dire consequences, particularly towards major livelihoods (rain-fed agriculture) that are reliant on the natural environment. The effect on livelihood has serious implications towards the realisation of Sustainable Development Goals (SDGs) such as SDG 1 (no poverty), SDG 2 (zero hunger), SDG 3 (good health and wellbeing), SDG 11 (sustainable cities), SDG 13 (climate action), and SDG 17 (partnerships for the goals).

Alongside the complex interaction between LULCC and its impact on enhancing greenhouse gas emissions, there are also seasonal winds that influence climate variations. In East Africa, large scale winds such as the Intertropical Convergence Zone (ITCZ) bring increased levels of rainfall to the equatorial region. On the global scale, winds like the La-Nina, El-Nino and the Indian Ocean Dipole also shape climatic variabilities and determine whether regions will experience wet or dry (drought) conditions (James and Washington, 2013). Regardless of these exceptionalities, LULCC has proven to have a significant impact on climatic variables (Zhou et al., 2015; Akpoti et al., 2016; Achugbu et al., 2021). The change in land cover alters soil moisture, thermal characteristics, surface textures and the albedo which influences climatic variables. These gradual changes also affect terrestrial hydrology which alters rainfall and evapotranspiration. Studies such as Klein et al. (2017) showed biosphere-precipitation feedback for the savanna region in West Africa. This has been attributed to the properties of energy (transitional) and water which makes them responsive to changes in land use. For example, in West Africa, the interaction between the land surface and its overlaying atmosphere determines the climate over a period of time given the high net radiation and moisture generating high evaporation rates.

To understand the interaction among LULCC, several scholars have employed land use models that account for how LULCC induces a change in elements such as surface textures, albedo, Bowen ratio and vegetation dynamics (Kidane et al., 2012; Chen and Dirmeyer, 2016; Rigden and Li, 2017; Wang et al., 2017; Burakowski et al., 2018). Others such as Hulme (1994) and Abbasian et al. (2019) also used the General Circulation Model (GCM) to quantify the effect of land use change on climatic variables such as precipitation. The same model has also been used by Taylor et al. (2002) and Yonaba et al. (2023) to model land use on precipitation outcomes in the Sahelian regions. This approach however produced limited results as Africa having low historical climate data affected its estimates, leaving scholars with no choice but to model prediction from global models which relegated predictions of Africa to a sub-grid scale status (Moore et al., 2015). In East Africa, Moore et al., (2015) argue that the GCMs establish a strong response to elevated GHGs and their impact on climatic variables such as temperature and rainfall. Most GCMs are good at predicting wetter conditions. These models are even considered accurate in scenarios where Coupled Model Intercomparison Project (CMIP) data is used. Despite the positive feedback on rainfed agriculture, the model's inability to reproduce (model) drying trends accurately posses threats to adaptive strategies designed to cushion small-scale farmers. This limitation is due to the model omitting regional-scale (SST changes) forcing trends such as the Pacific Ocean and Indian Ocean Sea Surface temperature. Moore et al., (2015) further acknowledge that rainfall variability is heavily influenced by large-scale circulations, which supports the use of GCMs. A focus on regional-scale climate impact is therefore recommended for decision making on the African continent. The GCMs thus become limited here as they are unable to make predictions for local scales with heterogeneous land covers. Similarly, James and Washington (2013) have argued that GCMs' inability to capture inconsistent changes in temperature due to variations in climate sensitivity and the feedback mechanism, limits its use on the regional scale compared with the global scale.

Using the medium of land surface-atmosphere interactions, Achugbu et al. (2021) adopted Charney's (1975) hypothesis on precipitation being responsive to the state of the vegetation to understand LULCC and climate change in West Africa. This hypothesis has however been affirmed and rejected by different studies that have obtained different outcomes. Affirming the hypothesis Swan (2012) and Yosef et al. (2018) have shown that afforestation enhances precipitation. However, this has been challenged by works conducted by Zhang and Wei (2021) who show that deforestation in forest regions results in high evapotranspiration which increases rainfall. In their perspective, afforestation in forest regions increases the forest canopy which reduces evapotranspiration and which reduces precipitation. Nevertheless, Achugbu et al. (2021) argue that the discrepancies observed in these model outcomes can be attributed to simulations performed using either different spatial resolutions or different LULC data. To address these challenges, scholars such as Yan et al. (2020) and Glotfelty et al. (2021) integrate remote sensing data and the Community Land Model respectively with the WRF model; this approach presents accurate results over the study regions.

More importantly, emerging trends and linkages established between LULCC and its associated implications on enhancing greenhouse gases (with a focus on temperature and precipitation), necessitate a prompt response. Despite growing awareness of climate change, significant knowledge gaps on climate trends in Africa remain due to several challenges. One major issue is the lack of reliable, long-term meteorological data, particularly in rural areas, where limited infrastructure like weather stations restricts data. For instance, many parts of West Africa have insufficient climate monitoring networks, which hinder precise

modeling of rainfall patterns crucial for agriculture. Additionally, climate variability across Africa's diverse regions, from the Sahel to coastal zones, requires localized models, but many studies rely on broad, global models that fail to capture these regional differences. For example, the IPCC has acknowledged that many global climate models struggle to accurately represent rainfall patterns in equatorial Africa (IPCC, 2021; Crétat et al., 2014). Furthermore, research funding and institutional capacity for climate studies are limited in many African countries, leading to a reliance on external data sources, which may not fully reflect local realities (Eriksen et al., 2021). This is compounded by urbanization, deforestation, and other environmental pressures, such as in Ethiopia, where rapid urban growth has exacerbated local climatic changes, including the urban heat island effect (Li et al., 2022). Collaboration between African nations on climate research also faces barriers due to political and economic constraints, limiting comprehensive, continent-wide climate models. Addressing these deficits is critical to developing climate resilience strategies tailored to Africa's diverse environments and socio-political realities.

To address these gaps in knowledge, this paper's main contribution is to explore the links between land cover change (LCC) and its socio-environmental and economic implications, as well as its undesirable effects on climatic variables such as temperature and precipitation. For instance, Houghton et al. (2012) examined how land-use changes, particularly deforestation and agricultural expansion, contribute to global carbon emissions, exacerbating climate change. Foley et al. (2011) further highlighted the broad environmental impacts of land cover change, including alterations in ecosystem services, biodiversity loss, and the regulation of water and energy cycles. This study fills crucial gaps by (i) widening the lens to capture land use, precipitation, and temperature trends for the entire continent of Africa from 1993 to 2023, (ii) establishing the causal influence between LULCC variables on temperature and precipitation across Africa, and (iii) making land use, temperature, and precipitation predictions based on current trends to address land management and sustainability concerns.

To achieve these aims, the study employs Artificial Neural Networks-Cellular Automata (ANN-CA) within MOLUSCE, Random Forest (RF), and Convergent Cross Mapping (CCM) to model the impacts of LULCC on temperature and precipitation across Africa. This integrated methodological approach improves upon previous models by capturing both predictive trends and causal relationships, which have often been overlooked in earlier studies. The ANN-CA model facilitates detailed LULCC simulations, RF enhances the precision of temperature and precipitation projections, and CCM helps establish robust causal linkages between LULCC and climatic variability. We reckon that modeling LULCC alongside climatic variables, particularly temperature and precipitation both of which have been predicted to increase the vulnerability of the continent will highlight patterns that are critical for the development and implementation of adaptive responses. Addressing these aims can help policymakers, particularly in countries where adaptation strategies are weaker, to develop targeted approaches for the upcoming years and decades. By gaining a better understanding of the rate of land cover change and its climatic effects, these countries can implement adaptation measures more effectively to mitigate negative impacts and enhance climate resilience. While the knowledge gained from this study will be valuable for policymakers across Africa, it will be especially beneficial for regions with limited resources and institutional capacity to respond to environmental challenges. In addition, the insights obtained can foster stronger collaboration within economic blocs such as ECOWAS and SADC, supporting regional efforts toward sustainable development, effective land management, and climate adaptation.

2. Study area and methods

2.1. Study area

Africa, the second-largest continent, covers approximately 30.37 million square kilometers and showcases a wide array of geographical features and ecosystems. Bordered by the Mediterranean Sea, Atlantic Ocean, Indian Ocean, and Red Sea, the continent is bisected by the Equator, resulting in diverse climates and landscapes. Key geographical highlights include vast deserts such as the Sahara, fertile river basins like the Nile and Congo, significant mountain ranges such as the Atlas and Drakensberg, and the tectonically active Great Rift Valley in Eastern Africa, renowned for its biodiversity. Temperature patterns vary significantly across the continent, with equatorial regions experiencing minimal seasonal variation and desert areas like the Sahara facing extreme temperature swings. Precipitation is also highly variable, influenced by factors such as the Intertropical Convergence Zone (ITCZ), mountains, and ocean currents, leading to abundant rainfall in equatorial regions, distinct wet and dry seasons in the savanna, and minimal rainfall in desert areas.

Africa was selected for this Land Use and Land Cover Change (LULCC) analysis due to its ecological diversity and pressing environmental challenges. The continent's varied ecosystems from tropical rainforests to arid deserts provide a unique opportunity to study how land use patterns evolve under different environmental conditions. Africa faces critical issues, including rapid urbanization, deforestation, and the severe impacts of climate change, such as rising temperatures and altered precipitation patterns (Oduro et al., 2022). These challenges have significant implications for biodiversity, food security, and sustainable development. By investigating LULCC in Africa, the study aims to identify the drivers of these changes and formulate effective land management and climate adaptation strategies. The findings will be valuable not only for Africa but also for other regions grappling with similar challenges.(Fig. 1)

2.2. Data acquisition and methodology

In this study, a total of thirty Landsat images with a 30-meter spatial resolution, covering the period from 1993 to 2023, were obtained from the Google Earth Engine. Landsat imagery was selected to achieve an optimal balance between spatial detail and temporal continuity, ensuring a consistent and comprehensive dataset for long-term LULCC analysis across Africa. To enhance the accuracy of the dataset, image preprocessing was conducted using ArcGIS 10.8 and ENVI 5.3, which involved radiometric calibration, atmospheric correction, layer stacking, and supervised classification. These preprocessing steps ensured that the images were free from distortions and ready for accurate land cover classification. For land cover classification, Landsat 5 TM (1993–2001) and Landsat 7 ETM+ (2002–2015) utilized bands 7, 4, and 2, while Landsat 8 OLI/TIRS (2016–2023) employed bands 7, 5, and 3 to optimize the detection of vegetation and built-up areas. Each satellite's specific row/path configurations were carefully applied to maintain spatial consistency across different time periods. In addition to land cover data, climate variables such as temperature and precipitation, measured at 2 m above the surface, were obtained from the fifth-generation European Centre for Medium-Range Weather Forecasts (ECMWF) Reanalysis (ERA5) database. Spanning 1993–2023, the ERA5 dataset provided high-resolution, globally consistent climate data, making it an ideal source for analyzing long-term temperature and precipitation trends in relation to land cover changes.

To further enhance the robustness of our analysis, we integrated land surface temperature (LST) and precipitation retrievals, allowing for a more comprehensive assessment of environmental changes and the impact of climatic factors on land cover transitions across Africa. Ensuring the reliability and consistency of input data for causality analysis was a key priority. Therefore, we carefully selected high-

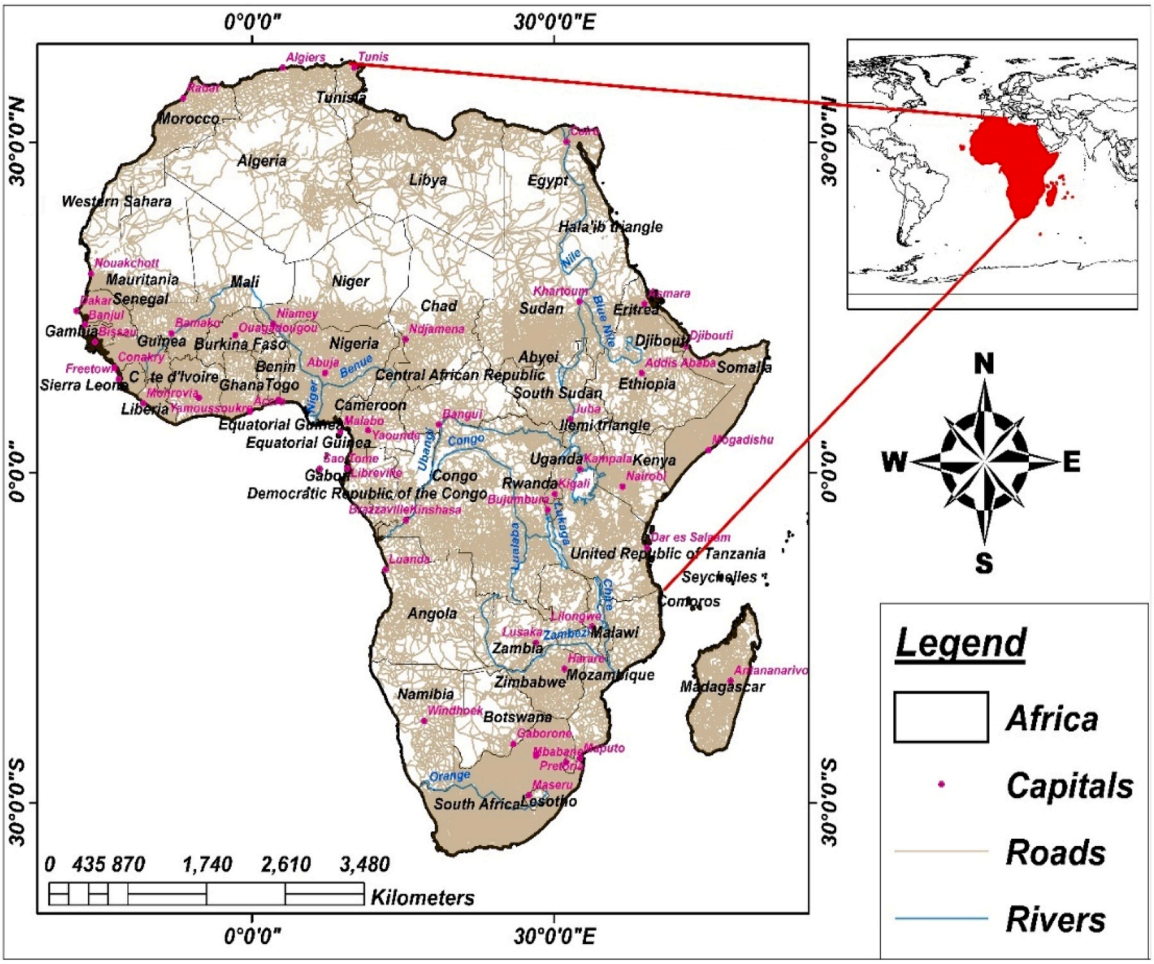

Fig. 1. Geographical location of study area.

quality, globally recognized datasets with proven accuracy for long-term LULCC and climatic assessments. The ERA5 reanalysis dataset was chosen for its advanced data assimilation techniques, which correct for observational gaps and provide reliable climate records. Similarly, Landsat-derived land cover datasets were employed due to their well-documented temporal consistency and classification accuracy. To mitigate uncertainties associated with historical data limitations, we implemented rigorous preprocessing techniques, including gap-filling, outlier removal, and cross-validation with alternative datasets where applicable. These steps ensured that the datasets used in our analysis were as comprehensive, accurate, and consistent as possible. While we acknowledge the inherent challenges of historical data availability in some remote regions of Africa, the combination of globally standardized datasets and robust preprocessing methods significantly reduced uncertainties, enhancing the reliability of our causal inference results. (Fig. 2)

2.2.1. Land cover classification and change analysis

Supervised image classification techniques were employed to categorize the land cover data into six distinct classes: built-up areas, forest, desert/bare land, farmlands, waterbodies, and grassland/shrublands (Table S.1). The classification process utilized the Maximum Likelihood Classification Algorithm (MLCA), a widely adopted parametric approach that assigns each pixel to the most probable land cover class based on Bayesian probability estimates (Mishra & Upadhyay, 2022). Prior to classification, the Landsat imagery underwent essential preprocessing steps, including radiometric calibration to correct sensor-specific distortions, atmospheric correction using the Dark Object Subtraction (DOS) method to remove atmospheric scattering effects, and geometric correction to ensure spatial alignment with reference datasets. Training samples for each land cover category were selected through ground truthing and high-resolution imagery validation, ensuring robust spectral separability between classes. The MLCA method then computed the probability distribution of spectral reflectance values within each class, leveraging covariance matrices to enhance classification precision. To further refine accuracy, a post-classification correction was applied using ancillary data and manual verification, minimizing misclassification errors and improving thematic consistency.

To ensure the accuracy and reliability of the land-use classifications, we conducted an extensive accuracy assessment using ground-truth validation. A total of 6000 validation points (1000 per land-use class) were randomly generated and stratified across different land cover types: desert/bare land, built-up areas, waterbodies, forests, farmlands, and grasslands/shrubs. These sampled points were overlaid onto high-resolution Google Earth Pro imagery and compared with in-situ land cover datasets from national and regional monitoring programs. The classification accuracy was evaluated using user's accuracy, producer's accuracy, and the Kappa coefficient, ensuring a robust assessment of classification consistency and reliability. Furthermore, we included confidence intervals for accuracy metrics to provide a more transparent evaluation of classification performance. These refinements enhance the robustness of our methodology and ensure that classification outputs accurately reflect LULCC trends across Africa.

A LULCC statistical analysis was conducted to evaluate the continuity of land use systems across Africa and to identify the key factors driving these changes. The analysis was guided by specific mathematical

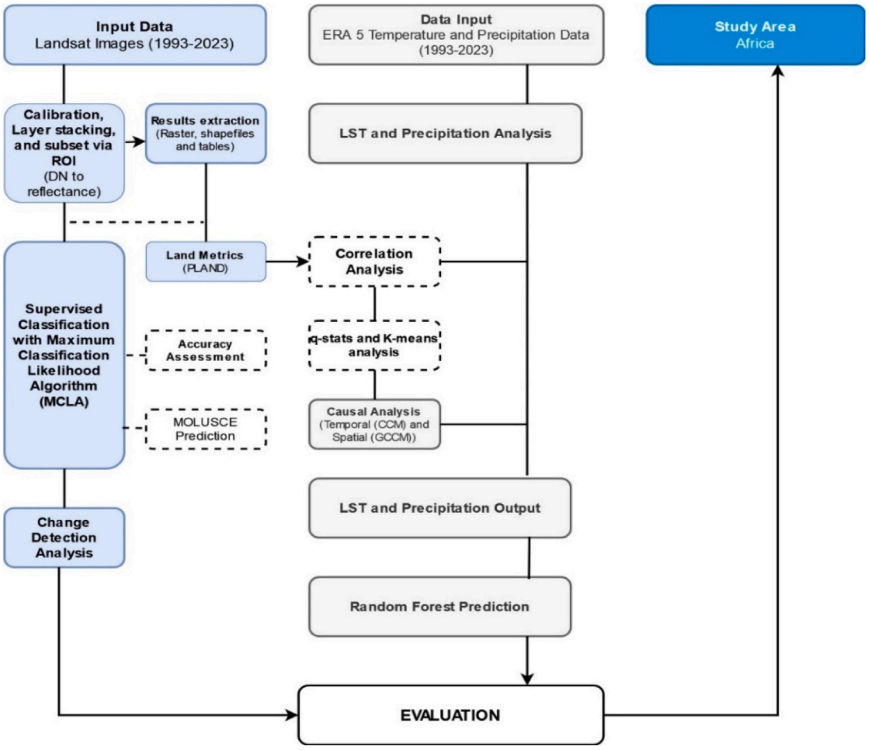

Fig. 2. Flowchart diagram of the study.

models and equations (Eqs. 1, 2, and 3) designed to quantify the extent of land cover transitions and the influence of various environmental, socio-economic, and climatic factors on these transitions. This approach enabled a comprehensive understanding of the dynamics of land use and land cover in Africa, revealing patterns of change and continuity over time and helping to pinpoint the underlying causes of these changes.

$$Change\ in\ LULCC = \frac{l-k}{k} \tag{1}$$

$$\%Change\ in\ LULCC = \frac{l-k}{k} x \quad 100\% \tag{2}$$

$$Rate\ of\ Change\ in\ LULCC\ per\ year = \left[\left(\frac{l-k}{k}\right)x \quad 100\%\right] \div t \tag{3}$$

Where the variable k represents the land use and land cover change (LULCC) for the previous year, while l denotes the LULCC for the current year. The variable t corresponds to the studied time span or interval. In this study, t represents the total duration of the analysis, which is 30 years, covering the period from 1993–2023. These variables are critical in the mathematical models used to assess and quantify the continuity and shifts in land use systems across Africa, allowing for a detailed examination of how land cover has evolved over the study period and identifying the factors that have influenced these changes.

2.2.2. Temperature analysis

2.2.2.1. Image calibration (Radiance). Radiometric correction was performed to address atmospheric effects and improve image clarity. This process included gap-filling for images exhibiting stripes or other artefacts and removing any distortions to ensure accurate data representation.

2.2.2.2. Digital number (DN) to radiance conversion. For Landsat imagery, which has DN values ranging from 0 to 255, the conversion to spectral radiance was carried out following the method outlined by Coll et al. (2009) and detailed in the USGS Landsat User Handbook. The conversion was executed using the provided mathematical formula to accurately calculate the radiance values for the study area. The analytical framework relied on the mathematical equations implemented in ArcGIS 10.8 (5) and (6) (Sarfo et al., 2023):

$$L_\lambda = \frac{(LMAX_\lambda - LMIN_\lambda)}{(QCALMAX - QCALMIN)} x(DN - QCALMIN) + LMIN_\lambda \tag{5}$$

where L_λ is cell value as radiance in $W/(M^2 * sr * \mu m)$; $LMAX_\lambda$ is the sensor spectral radiance that is scaled to $(QCALMAX)$ in $W/(M^2 * sr * \mu m)$; $LMIN_\lambda$ is the sensor spectral radiance that is scaled to $(QCALMIN)$ in $[W/(M^2 * sr * \mu m)]$. $(QCALMAX)$ is the maximum quantized calibrated pixel value to $LMAX_\lambda$ [DN], $(QCALMIN)$ is the minimum quantized calibrated pixel value corresponding to $LMIN_\lambda$ [DN]; and QCAL is the quantized calibrated pixel value [DN]. Equation 4 can be observed from header files ETM+ and TM datasets from the USGS website. The LMIN and LMAX are the spectral radiances for each band at digital numbers (DN) 1 and 255 for Landsat 7 ETM+ , 1 and 65535 for Landsat 8 OLI/TIRS. λ is the wavelength. This was done using ArcGIS 10.8 using the below formula:

$$LST = \left(\frac{K_2}{\ln\left(\frac{K_1}{Radiance+K_0}+1\right)}\right) - 273.15 \tag{6}$$

where LST denotes Land Surface Temperature in degrees Celsius (°C). Radiance is the degree of emissivity observed by the sensor. K_0, $K_1 and K_2$ are constants associated with sensor calibration. To validate the accuracy of the temperature estimates derived from the Landsat images, we conducted a comparative analysis with temperature data obtained from the ERA5 reanalysis dataset for the corresponding years. The ERA5 data, known for its high-resolution and reliability, served as a benchmark for this comparison. After preprocessing and aligning the temporal and spatial resolutions of both datasets, statistical analysis was performed to assess the consistency between the Landsat-derived

temperatures and the ERA5 measurements. The results indicated no significant difference between the two datasets, thereby affirming the reliability of the temperature estimates obtained from the Landsat imagery. This validation step strengthens the confidence in the methodology and supports the argument that remote sensing data can be effectively used for accurate temperature analysis over time.

2.2.3. Precipitation analysis

To analyze precipitation using ERA5 reanalysis data, the process began by acquiring high-resolution precipitation datasets from the European Centre for Medium-Range Weather Forecasts (ECMWF), covering the period from 1993 to 2023. The raw data were preprocessed to align with the study area's spatial and temporal resolutions, including interpolation and quality control measures to address missing values and outliers. The precipitation analysis involved calculating average precipitation and spatiotemporal variations. Spatial analysis was conducted and the results were visualized through maps. Expressions related to landscape metrics (Equation S1), q-statistics (Equation S2) and K-means analysis of LULCC variable, temperature and precipitation are captured in the supplementary file. Similarly, details about the causality approach utilized in this study are presented in the supplementary material (Equations S3-S11).

2.3. Prediction

2.3.1. LULCC prediction

Projections for the years 2033, 2043, and 2053 were generated using the Modules for Land Use Change Evaluation (MOLUSCE) in QGIS version 2.18, employing Cellular Automata and Artificial Neural Network (CA-ANN) methodologies to simulate future land use and land cover change (LUCC) patterns across Africa. These simulations leveraged historical LUCC data from 1993 to 2023, allowing for the assessment of long-term land transformation trends. The analysis was guided by Evaluating Correlation (EC) metrics, spatial area transitions, and Transition Potential Computation (TPC) modeling, all validated through three iterative cycles to ensure robustness.

The modeling process was underpinned by critical reference datasets, including a high-resolution Digital Elevation Model (DEM) with a spatial resolution of 30 m, providing detailed topographical insights essential for understanding elevation-related impacts on land use and climate. Additionally, a georeferenced road network raster of Africa with a 100-meter resolution was incorporated to accurately analyze the influence of transportation infrastructure on land cover changes. To improve predictive accuracy, the model integrated key predictor variables, including built environment dynamics (change likelihood, developed land density, cropland extent, and proximity to transportation networks), socio-economic indicators (population density, household numbers, urbanization rates, and industrial growth), and natural environment parameters (climatic variables such as temperature and precipitation with a monthly temporal resolution, soil moisture, and ecological features such as vegetation indices). These factors, combined with topographical characteristics derived from the DEM, provided a comprehensive framework for predicting LUCC patterns with greater precision, especially in the diverse and rapidly changing landscapes of Africa (Sarfo et al., 2023).

To ensure the reliability of future land use simulations, a rigorous calibration and validation process was conducted for the MOLUSCE and ANN-CA models. The calibration phase involved training the ANN-CA model using historical LUCC data from 1993 to 2023, with transition probabilities derived from observed land cover transformations over the study period. Key driving factors, including topography, proximity to roads, population density, and land use zoning regulations, were incorporated to enhance the model's predictive capabilities. Model parameters were iteratively optimized using transition potential modeling to achieve the best performance. For validation, we simulated the 2023 land cover map using historical data from 1993 to 2013 and compared the predicted outputs with the actual 2023 classified land cover. The accuracy of the predicted land cover was evaluated using Kappa statistics and Overall Accuracy which measures the degree of agreement between observed and simulated land cover. The validation results confirmed the model's ability to capture historical LUCC trends, thereby strengthening the 2033–2053 projections and ensuring the reliability of our future land cover simulations.

2.3.2. Temperature and precipitation prediction

In this study, the Random Forest (RF) algorithm was employed to predict temperature and precipitation trends in Africa for the years 2033, 2043, and 2053. The RF model was selected for its robustness and accuracy in handling large datasets with complex interactions, as well as its ability to manage nonlinear relationships between predictor variables. The prediction process involved training the RF model using historical climate data (1993–2023), including temperature and precipitation records, alongside relevant land use and land cover (LULC) variables derived from remote sensing data.To ensure accurate and generalizable predictions, the model was calibrated using a set of independent variables, including historical LULC data, Digital Elevation Models (DEMs), vegetation indices, and socio-economic factors such as population density and urbanization rates. The training process involved generating multiple decision trees, each built from a randomly selected subset of the data, and then aggregating these results to form the final prediction. To further improve model reliability, we implemented 10-fold cross-validation and hyperparameter tuning, optimizing key parameters such as the number of trees, maximum depth, and minimum sample splits to prevent overfitting or underfitting. Additionally, out-of-bag (OOB) error estimates were used to evaluate the model's generalizability, ensuring predictions were not overly sensitive to training data.

For the prediction of future climate conditions, the calibrated RF model was applied to forecast temperature and precipitation for the target years by incorporating projected LULC changes, which were themselves generated using the Cellular Automata and Artificial Neural Network (CA-ANN) approach within the MOLUSCE module in QGIS. This integration provided a dynamic view of how alterations in land use and land cover might influence climate variables over time. To further enhance the robustness of these projections, we conducted feature importance analysis and sensitivity assessments. Feature importance was ranked using Gini impurity and permutation importance scores, identifying land cover types, elevation, historical temperature/precipitation trends, and vegetation indices as the dominant factors shaping future climate patterns. A sensitivity analysis was conducted by systematically varying input parameters and assessing their impact on model outputs, providing deeper insights into the stability and reliability of our projections. The results from the RF model were analyzed to identify spatial and temporal patterns in temperature and precipitation across Africa, highlighting potential climate hotspots and regions at risk of extreme weather events. The formula for a RF prediction model, specifically for temperature and precipitation prediction, can was summarized as follows:

2.3.3. Individual decision tree prediction

For each tree t in the forest (where t = 1,2,…,T and T is the total number of trees as expressed in Eq. 7):

$$\widehat{Y}_t(X) = f_t(X) \tag{7}$$

where X represents the input features (historical temperature, precipitation, land use), $\widehat{Y}_t(X)$ is the predicted value of the response variable (e.g., temperature or precipitation) from the t^{th} decision tree, and $f_t(X)$ is the prediction function of the t^{th} tree, which is a non-parametric function learned from the data.

Random Forest Ensemble Prediction is expressed as (Eq. 8):

$$\widehat{Y}_{RF}(X) = \frac{1}{T}\sum_{T=1}^{T}\widehat{Y}_t(X) \quad (8)$$

where $\widehat{Y}_{RF}(X)$ is the final predicted value for the response variable (temperature or precipitation) using the Random Forest model. The summation aggregates the predictions of all T decision trees, and the average provides the ensemble prediction.

2.3.4. Model performance and validation

The model performance was evaluated using ANN-CA from MOLUSCE, RF, and CCM to assess their predictive accuracy in temperature and precipitation projections across Africa. The ANN-CA model, implemented within the MOLUSCE plugin in QGIS, was used for LULCC modeling, while RF was applied for LST and precipitation predictions, and CCM was used to analyze the causal relationships between LULCC and climate variables. Model accuracy was assessed using three key statistical metrics: coefficient of determination (R^2) to measure the goodness of fit, root mean square error (RMSE) to quantify deviations from observed values, and mean absolute error (MAE) to evaluate the average prediction error. These metrics were computed by comparing the predicted climate values against historical satellite-based climate records, ensuring a robust validation of the models' predictive capabilities.

3. Results

3.1. Analysis of Africa's land use and land cover change

Table 1 and Fig. 3 depict the spatial trends of Land Use and Land Cover Change (LULCC) in Africa for the years 1993, 2003, 2013, and 2023. The data reveal that in 1993, forests and deserts/bare lands were the most prevalent land cover types, followed by grasslands and shrubs, particularly in the eastern, central, and western regions of the continent. By 2013, there was a noticeable increase in built-up areas, which progressively encroached upon deserts and farmlands. This expansion of urban environments can be attributed to historical patterns of urbanization and economic development, as well as theories such as the "urban-rural divide" and the "pull or push theory" discussed in studies by Xiao et al. (2022) and Marchant et al. (2018). These theories highlight the socio-economic forces driving the significant transformation of land use across Africa, particularly in the post-independence era, where land was increasingly developed for residential, commercial, educational, and agricultural purposes. Consequently, the expansion of built-up areas over the past 30 years has led to a reduction in grasslands/shrublands, farmlands, and deserts, reflecting the continent's rapid urbanization and the growing demand for land resources. The continuous increase in urban areas underscores the dynamic nature of LULCC in Africa and its implications for sustainable development and environmental conservation.

3.1.1. Temporal variations of LULCC in Africa

Table 2 illustrates the temporal variations in Land Use and Land Cover (LULC) across four distinct time periods: 1993–2003, 2003–2013, 2013–2023, and the cumulative period from 1993 to 2023. Over the past four decades, Africa has undergone significant transformations in its land use patterns. Notably, there has been a dramatic increase in built-up areas (+134 %) and waterbodies (+71 %). This expansion reflects the continent's rapid urbanization and infrastructure development, as well as changes in hydrological systems. Interestingly, the data also indicate a modest regrowth in forested areas (+2.61 %), suggesting some success in reforestation efforts or natural forest recovery. However, this positive trend contrasts with the decline observed in other land cover types, such as deserts (-12.29 %), farmlands (-14.53 %), and grasslands/shrubs (-14.20 %). These reductions are largely due to the conversion of these lands into urban areas, reforested zones, or areas that have become waterlogged. These shifts highlight the complex dynamics of land use in Africa, where environmental, socio-economic, and climatic factors are driving significant changes across the continent. The analysis of land cover changes in Africa over the past thirty years has revealed significant trends. An overall accuracy rate of 96 %—calculated from producer, user, and kappa accuracies—demonstrates a high level of precision in assessing these temporal dynamics for the years 1993, 2003, 2013, and 2023 (Fig. S.).

Table 3 presents statistics for the rate and magnitude of change, in relation to LULCC in Africa over the past 30 years.

Table 3 shows that farmlands, deserts, and grasslands/shrubs experienced annual decreases of 0.48 %, 0. 41 %, and 0. 47 %, respectively. Conversely, built-up areas, forests, and regions covered by waterbodies saw annual increases of 4.49 %, 0.09 %, and 2.39 %, respectively. These trends reflect the ongoing transformation of Africa's landscapes, driven by urbanization, reforestation efforts, and changing hydrological patterns. The temporal dynamics of land cover alterations also unveiled substantial patterns. Built-up areas exhibited a considerable overall change magnitude increase of 1452,294 km^2 between 1993 and 2023, corresponding to an average annual change rate of 48,410 km^2, signifying the profound influence of urban development. Farmlands experienced a noteworthy decrease in change magnitude, totaling 517,274 km^2, with an average annual change rate decrement of 0.48 %. Forest cover observed a notable increase in change magnitude, amounting to 364,457 km^2, with an average annual change rate increment of 0.09 %. Waterbodies displayed a discernible overall change magnitude increase of 219,27 km^2, corresponding to an average annual change rate increment of 2.39 %. Notably, bare land witnessed a striking decrease in change magnitude of 724,325 km^2, with an average annual change rate decrement of 0.41 %, indicative of substantial land transformation processes such as deforestation, agricultural expansion, or urbanization.

3.2. Temperature analysis results

The temperature map of Africa from 1993, 2003, 2013, and 2023, as depicted in Fig. 4, demonstrates significant temporal and spatial variations in surface temperature across the continent over the past three decades. The temperature range has shown a consistent upward trend, with the highest recorded temperature increasing from 28.93°C in 1993–31.66°C in 2023, and the lowest temperatures fluctuating slightly from 5.88°C in 1993–7.29°C in 2023. This trend highlights a general warming of the continent, with a notable increase in temperature extremes over time. In 1993, the map shows a relatively broad distribution of moderate temperatures, with higher temperatures (28.93°C) concentrated in the northern regions, particularly in the Sahara Desert, while cooler temperatures (5.88°C) were prevalent in the highlands of East Africa and parts of Southern Africa. By 2003, the highest temperature rose to 29.64°C, and the spatial distribution of warmer temperatures expanded, particularly in the eastern parts of the continent. This period marks the beginning of a more pronounced warming in East Africa and the Sahel region, while the coastal and highland areas remained relatively cooler.

Table 1
Area coverage (sq.km) for LUCC in Africa (1993–2023).

Classes	1993	2003	2013	2023
Farmlands	3559,116	4451,938	4627,173	3041,842
Desert/Bareland	5893,299	5200,863	5003,458	5168,974
Built-Up	1078,742	1293,155	1397,324	2531,036
Grasslands/ Shrublands	5592,884	5158,041	5165,026	4798,460
Forests	13,939,830	13,938,008	13,935,578	14,304,287
Waterbodies	306,130	327,996	241,442	525,401
Farmlands				

***Total area coverage (Km^2) (Absolute) = 30,370,000

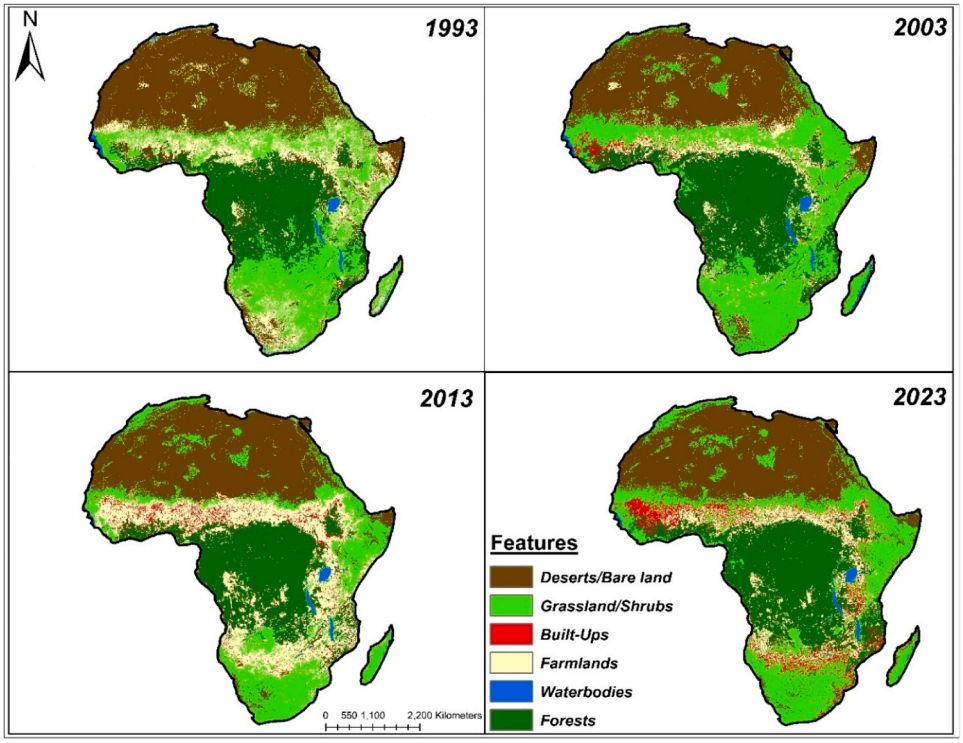

Fig. 3. LULCC over the past 30 years in Africa.

Table 2
Land cover changes between the given study periods (%).

Classes	1993–2003	2003–2013	2013–2023	1993–2023
Farmlands	+ 25.09	+ 3.94	−34.26	−14.53
Desert/Bareland	−11.75	−3.80	+ 3.31	−12.29
Built-Up	+ 19.88	+ 8.06	+ 81.13	+ 134.63
Grasslands/ Shrublands	−7.77	+ 0.14	−7.10	−14.20
Forests	−0.01	−0.02	+ 2.65	+ 2.61
Waterbodies	+ 7.14	−26.39	+ 117.61	+ 71.63

By 2013, the temperature range had further increased, with the highest recorded temperature reaching 30.52°C and the lowest temperature recorded at 6.91°C. The warming trend continued, with more areas in the northern and central parts of the continent experiencing higher temperatures. The spatial distribution of heat intensified in the Sahel and parts of East Africa, indicating a shift towards more extreme temperatures in these regions. The cooler regions, particularly in Southern Africa and the East African highlands, experienced slight temperature increase but remained cooler compared to the northern and central parts of the continent. In 2023, the highest temperature recorded was 31.66°C, with the lowest at 7.29°C. The map shows a significant expansion of high temperatures across the continent, with the most notable increases in the northern regions and the Sahel, where temperatures are consistently above 30°C. The warming is also evident in parts of West Africa and Central Africa, where previously moderate temperatures have now reached higher levels. The cooler regions, represented by blue and green hues, have also experienced warming, though they remain the coolest areas on the continent.

3.3. Precipitation analysis results

The precipitation map of Africa for the years 1993, 2003, 2013, and 2023 in Fig. 5 illustrates the significant changes in rainfall patterns across the continent over the past three decades. These maps reveal both the temporal and spatial variations in precipitation, highlighting areas of increased or decreased rainfall and providing insights into shifting climatic patterns. In 1993, the map shows a precipitation range with a maximum of 391.53 mm, concentrated primarily in Central and Southern Africa. The regions with the highest rainfall include the Congo Basin, parts of East Africa, and Madagascar. These areas, depicted in dark green and blue hues, contrast sharply with the arid regions of North Africa and the Sahara, where precipitation is virtually non-existent (0.00 mm). The concentration of rainfall in the central parts of the continent is consistent with the typical equatorial and tropical climate zones known for high annual precipitation.

By 2003, there is a noticeable shift in the precipitation pattern, with the highest recorded rainfall increasing dramatically to 752.32 mm. The areas with the most significant rainfall are still located in Central and Southern Africa, but the intensity and spread of these regions have expanded, particularly in East Africa and the coastal regions. The

Table 3
Rate and magnitude of change (sq.km) of LULCC in Africa (1993–2023).

Classes	1993 (sq.km)	2023 (sq.km)	Magnitude of change (sq.km)	Magnitude of change (sq.km)/year	Annual Rate of change (%)
Farmlands	3559,116	3041,842	−517,274	−17,242	−0.48
Desert/Bareland	5893,299	5168,974	−724,325	−24,144	−0.41
Built-Up	1078,742	2531,036	+ 1452,294	+ 48,410	+ 4.49
Grasslands/Shrublands	5592,884	4798,460	−794,424	−26,481	−0.47
Forests	13,939,830	14,304,287	+ 364,457	+ 12,149	+ 0.09
Waterbodies	306,130	525,401	+ 219,271	+ 7309	+ 2.39

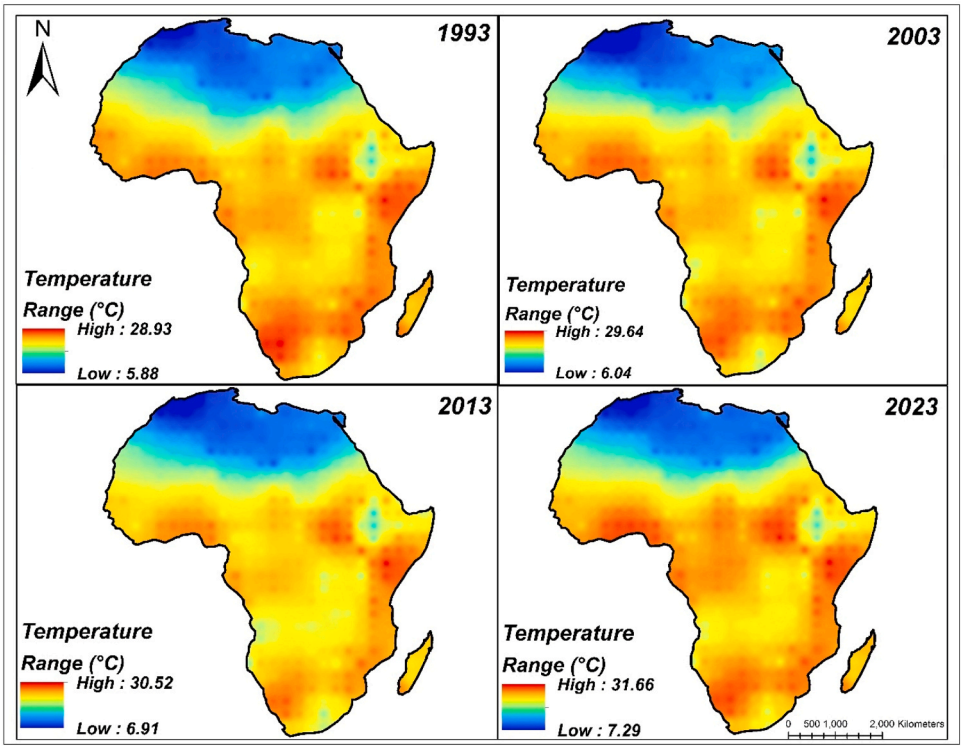

Fig. 4. Annual average LST variations in Africa (1993–2023).

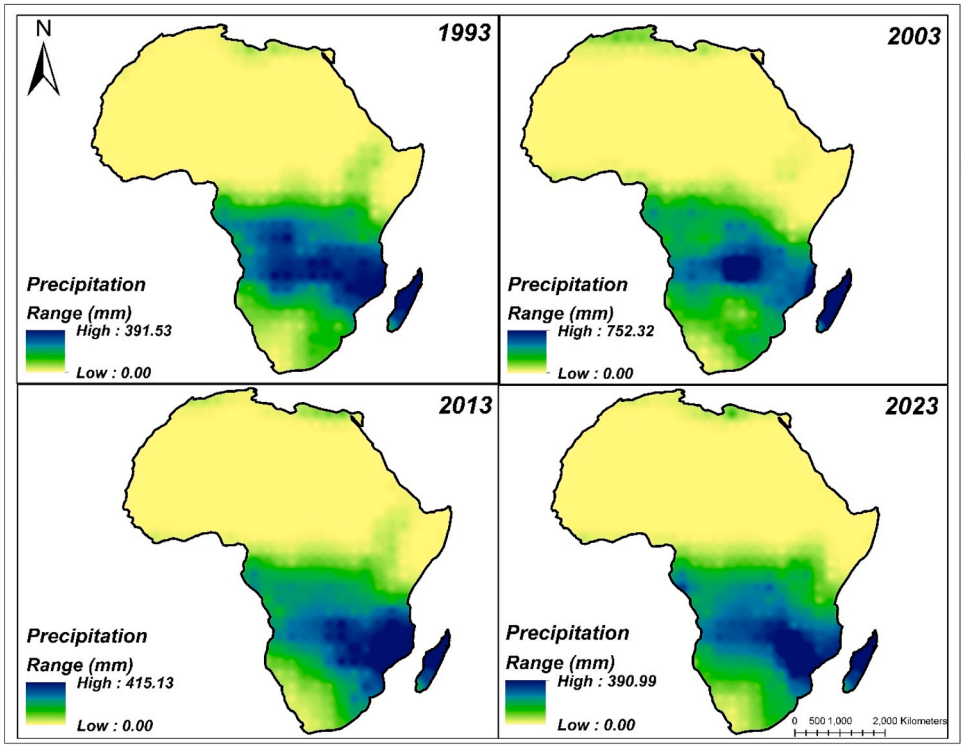

Fig. 5. Annual average Precipitation variations in Africa (1993–2023).

increase in precipitation is likely associated with enhanced tropical rainfall systems, possibly influenced by regional climatic phenomena such as the Indian Ocean Dipole or the El Niño-Southern Oscillation (ENSO). In 2013, the maximum recorded precipitation decreased to 415.13 mm, indicating a reduction in rainfall intensity compared to 2003. The spatial distribution of precipitation remains concentrated in the central and southern parts of the continent, but the areas with high rainfall have slightly contracted. This period may reflect a return to more typical rainfall patterns following the anomalous increase observed in the early 2000s. However, some regions, particularly in East

Africa, continue to receive substantial rainfall, though the overall intensity is lower than in 2003.

By 2023, the precipitation range has further decreased, with the highest recorded rainfall at 390.99 mm, comparable to levels seen in 1993. The map shows a continued concentration of rainfall in Central and Southern Africa, with the Congo Basin and parts of East Africa remaining as the primary regions of significant precipitation. The spatial distribution suggests a stabilization of rainfall patterns, though the overall trend indicates a slight decrease in precipitation intensity across the continent. These precipitation trends reflect the complex and dynamic nature of Africa's climate, influenced by various factors including regional and global climatic changes. The fluctuations in rainfall patterns have critical implications for water resources, agriculture, and ecosystem sustainability across the continent. The observed decrease in precipitation in some regions, particularly in the latter years, may signal emerging challenges related to water scarcity and drought, especially in areas already vulnerable to climate variability. Conversely, the increased rainfall in certain periods may lead to challenges such as flooding and soil erosion, necessitating adaptive strategies to manage these climatic extremes effectively.

3.4. Landscape metrics, temperature and precipitation

The correlation matrices presented in Fig. 6 illustrate the relationships between land use and land cover change (LULCC) variables, land surface temperature (LST), and precipitation. The first matrix highlights a strong positive correlation (0.868) between built-up areas and LST, indicating that increased urbanization leads to higher temperatures, reflecting the urban heat island effect. In contrast, forests show a significant negative correlation (-0.773) with LST, suggesting that dense vegetation contributes to cooler temperatures through transpiration and shading. Similarly, water bodies (-0.690), farmlands (-0.707), and grasslands/shrubs (-0.579) are associated with lower LSTs, while deserts and bare land exhibit a moderate positive correlation (0.495) with higher temperatures due to their lack of vegetation.

The second matrix examines the relationship between LULCC variables and precipitation. Forests demonstrate the strongest positive correlation with precipitation (0.716), indicating that areas with extensive tree cover tend to receive more rainfall, likely due to their influence on local microclimates. Farmlands and grasslands/shrubs also show positive correlations (0.665 and 0.556, respectively), suggesting that vegetated areas contribute to increased precipitation levels. Conversely, built-up areas have a strong negative correlation (-0.836) with precipitation, indicating that urban regions receive less rainfall due to landscape alterations. Deserts and bare lands also reflect a negative correlation (-0.481) with precipitation, consistent with their arid conditions. Interestingly, water bodies show a positive correlation (0.667) with precipitation, highlighting their role in influencing local humidity and rainfall patterns.

3.5. q-statistics and K-means analysis results of LULCC variable, temperature and precipitation

3.5.1. q-statistics results of LULCC variable, temperature and precipitation

The maps in Figure S.1 illustrate the q-statistics for the change in LULCC variables relative to changes in LST (ΔT) and precipitation (ΔP). A significant positive correlation is observed in northern Africa, particularly in the Sahara Desert (Fig.S.1a), where increasing desert/bare land areas correspond with rising temperatures, as barren landscapes absorb more heat. Additionally, urbanization shows a strong positive correlation with LST in West and East Africa, reflecting the urban heat island effect (Fig.S.1c). Conversely, dense forest (Fig.S.1 g) cover and significant water bodies (Fig.S.1k) are associated with negative correlations with temperature, particularly in central and southern Africa, where they help mitigate heat. In terms of precipitation, a strong negative correlation is evident in arid regions (Fig.S.1b), especially northern Africa, where desertification leads to decreased rainfall. While urbanization disrupts local hydrological cycles and may reduce precipitation in West Africa, some East African areas show a slight positive correlation due to localized microclimatic effects. Forested regions (Fig. S.1 h), particularly in the Congo Basin, generally correlate positively with precipitation, as dense forests enhance rainfall through evapotranspiration.

3.5.2. K-means results of LULCC variable, temperature and precipitation

The K-means clustering analysis (Fig. S.2) of ΔT and ΔP in relation to LULCC reveals distinct spatial patterns across Africa. Clusters 1 through 6 highlight regional responses to LULCC variables such as deforestation, urbanization, and agricultural expansion. Cluster 1, primarily in northern Africa, exhibits moderate temperature increases linked to the conversion of natural vegetation to desert/bare lands (Fig. S.2a, c, e, g, i, l) and urban areas, resulting in a slight decline in precipitation due to

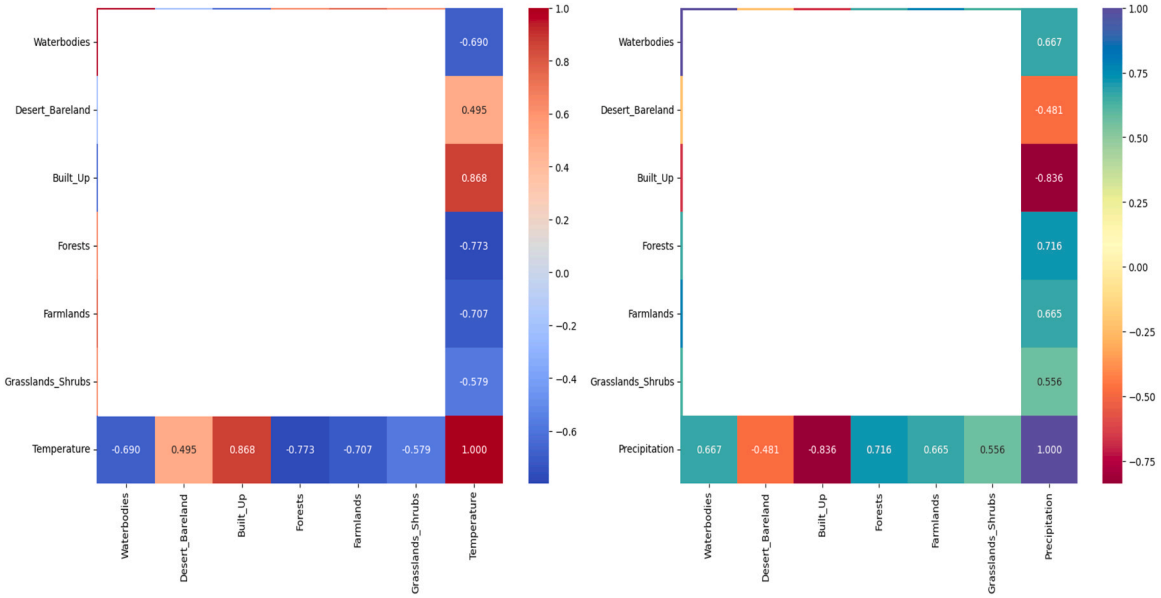

Fig. 6. Correlation between the Land cover types, Temperature and Precipitation.

reduced vegetative cover and altered hydrological cycles. In contrast, Cluster 2, spanning parts of West and East Africa, shows significant increases in both temperature and precipitation (Fig. S.2b, d, f, h, j, k), attributed to land cover transitions from grasslands and shrublands to agricultural fields and urban spaces, where enhanced evapotranspiration contributes to higher rainfall. Cluster 3, located in central and southern Africa, reports a more subdued temperature rise but notable increases in precipitation, likely due to preserved forest cover and reforestation efforts that enhance local moisture through recycling and increased humidity. Clusters 4, 5, and 6 demonstrate varied responses to LULCC, with Cluster 4 experiencing moderate temperature increases and variable precipitation patterns associated with farmland expansion. Meanwhile, Clusters 5 and 6 reflect complex interactions influenced by localized factors such as topography, land management, and proximity to water bodies.

3.6. Temporal and spatial causal inferences between temperature, precipitation and LULCC variables

The CCM analysis results in Fig. 7 and Fig. 8 provide insight into the directional causality between land use and land cover change variables and climate variables such as temperature (Temp) and precipitation (Precip). The results illustrate the extent to which changes in LULCC drive alterations in temperature and precipitation patterns across various ecosystems. The GCCM results in Figs. 9, 10, 11 and 12 on the other hand, provide a spatial perspective on the causal relationships between LULCC variables and climate variables (temperature and precipitation) across the African continent. The causality framework, based on CCM and GCCM, is designed to infer direct causal relationships between LULCC and climatic variables. Unlike traditional regression-based models that may be influenced by external factors, CCM and GCCM establish causality by reconstructing the state space of interacting variables, ensuring that only true causal links are detected. In this study, LULCC directly influences temperature and precipitation through well-established biophysical processes such as changes in surface energy fluxes, albedo, and evapotranspiration. External factors such as urbanization and industrialization are not confounders but rather intrinsic components of land cover change, captured within the LULCC framework itself. For instance, urban expansion is classified as a land cover category (built-up areas), and its influence on climate variables is analyzed as part of the LULCC-induced changes rather than as an external confounder. This ensures that the detected causal relationships are truly driven by land cover changes rather than by extraneous variables. The following sections analyze these relationships for different land cover types and their corresponding impacts on temperature and precipitation.

3.6.1. Temporal causal inference: temperature and LULCC variables

The CCM results show a steadily increasing correlation between built-up areas and temperature, with ρ values rising from approximately 0.1 at the beginning to almost 0.95 by time step 30. This strong positive correlation indicates that as urban areas expand, the local temperature increases significantly, confirming the urban heat island (UHI) effect. The UHI effect is driven by the replacement of natural land covers with impervious surfaces, which absorb and retain more heat, leading to higher surface and air temperatures. This trend is particularly evident in regions experiencing rapid urbanization, where the reduction in vegetation and increased anthropogenic heat emissions contribute to temperature amplification. The near-linear increase in ρ over time emphasizes the persistent and growing influence of urbanization on temperature, suggesting that unless urban development is managed sustainably, this trend will continue to exacerbate local warming. The causality between desert/bare lands and temperature also shows a strong positive trend, with ρ values reaching approximately 0.65 by time step 30. This suggests that areas transitioning to desert or bare land conditions are associated with significant temperature increases. The loss of vegetative cover in these regions reduces the cooling effect provided by plants through evapotranspiration, leading to higher surface temperatures. Additionally, the increase in surface albedo in bare lands reflects more solar radiation back into the atmosphere, which can

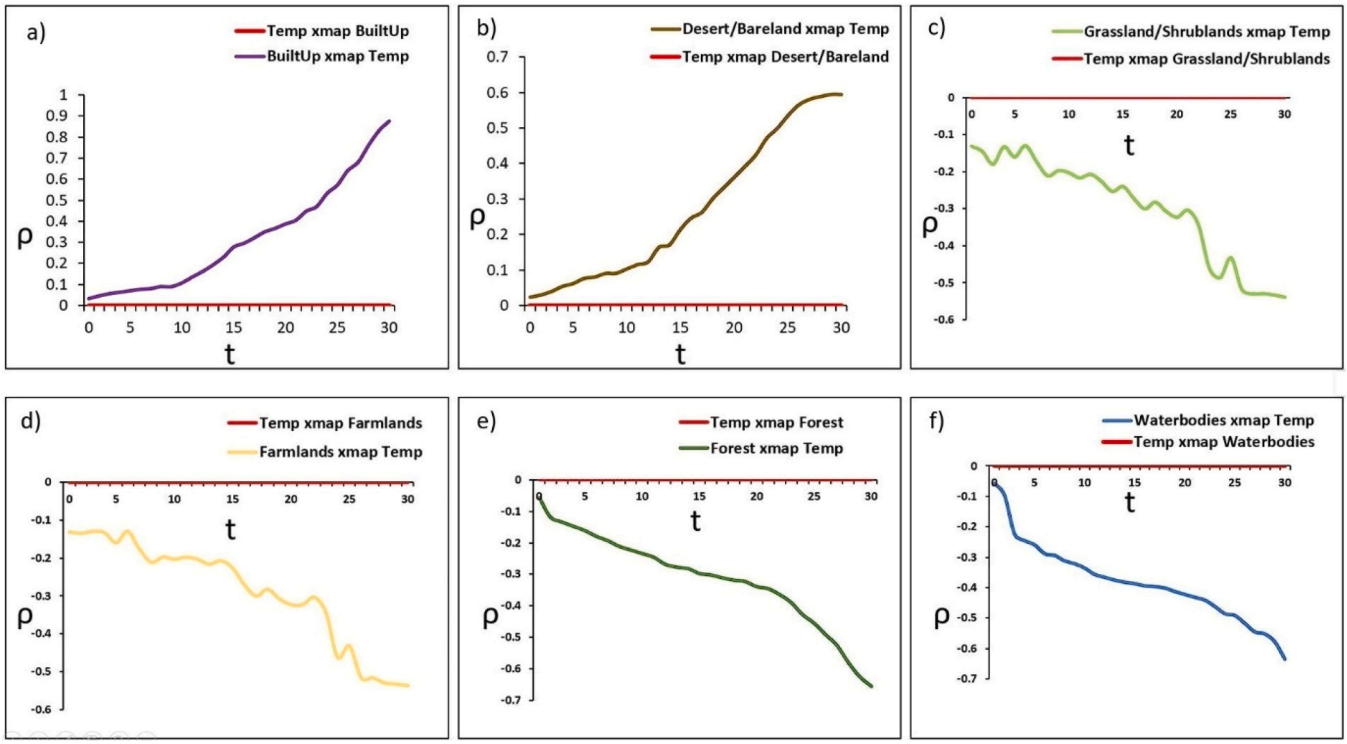

Fig. 7. CCM outputs of (a) Built Up and Temp; (b) Desert/Bareland and Temp; (c) Grassland/Shrubland and Temp; (d) Farmlands and Temp (e) Forests and Temp and (e) Waterbodies and Temp, t represents time, and ρ depicts the Cross-mapping Skill values.

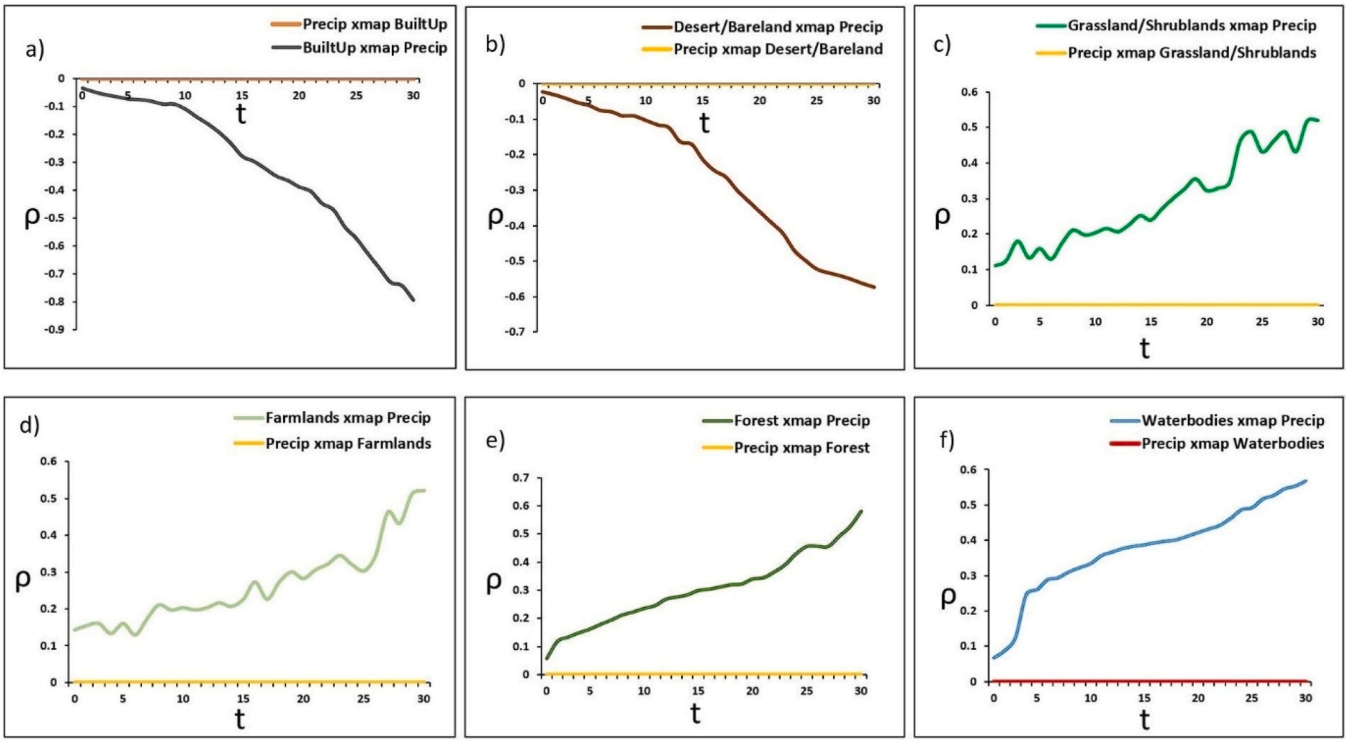

Fig. 8. CCM outputs of (a) Built Up and Precip; (b) Desert/Bareland and Precip; (c) Grassland/Shrubland and Precip; (d) Farmlands and Precip (e) Forests and Precip and (e) Waterbodies and Precip, t represents time, and ρ depicts the Cross-mapping Skill values.

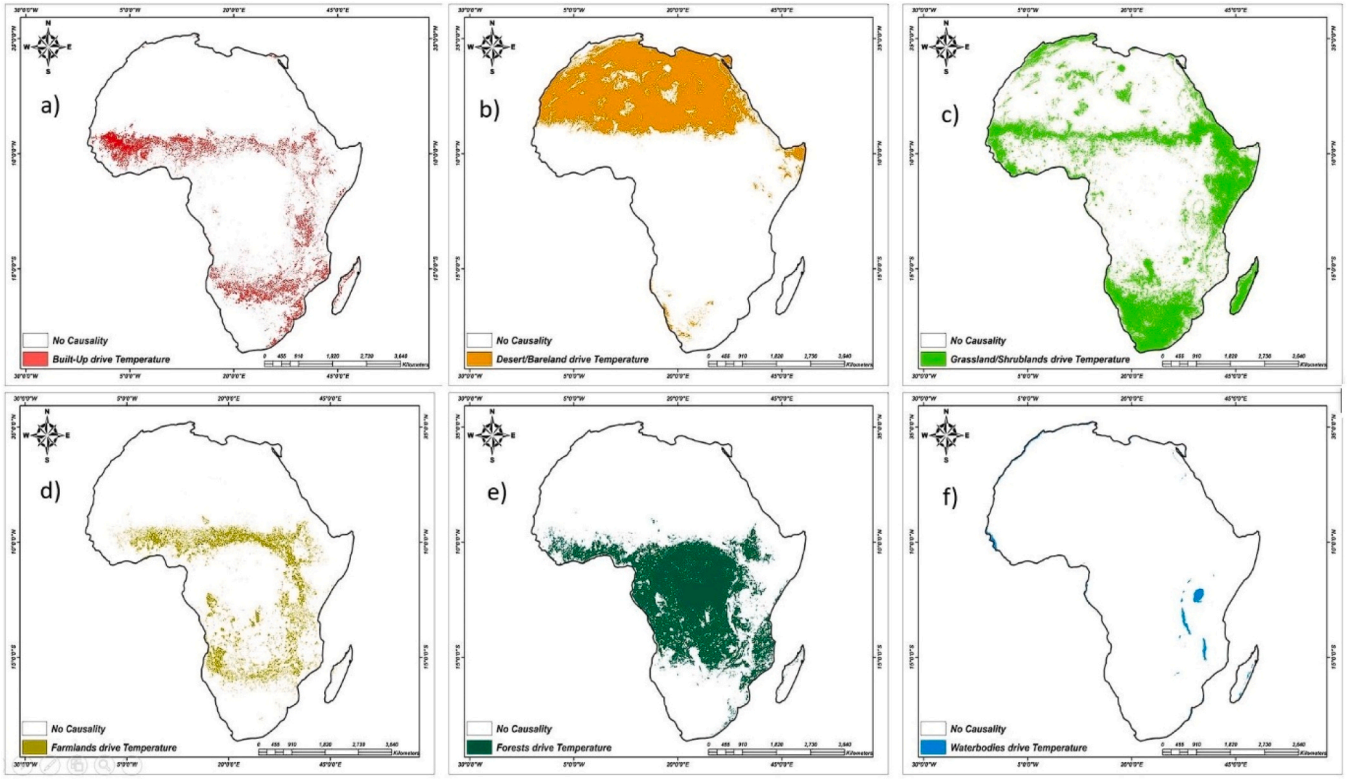

Fig. 9. GCCM Output (a) Built Up and Temp; (b) Desert/Bareland and Temp; (c) Grassland/Shrubland and Temp; (d) Farmlands and Temp (e) Forests and Temp and (e) Waterbodies and Temp and ρ depicts the Cross-mapping Skill values.

contribute to warming. The steady increase in the cross-prediction skill values (ρ) over time indicates that the expansion of desert/bare lands is a critical driver of temperature rise in these regions, highlighting the need for interventions such as reforestation and sustainable land management to combat desertification and its climate impacts.

The CCM analysis in Fig. 7 also shows negative cross-prediction skill

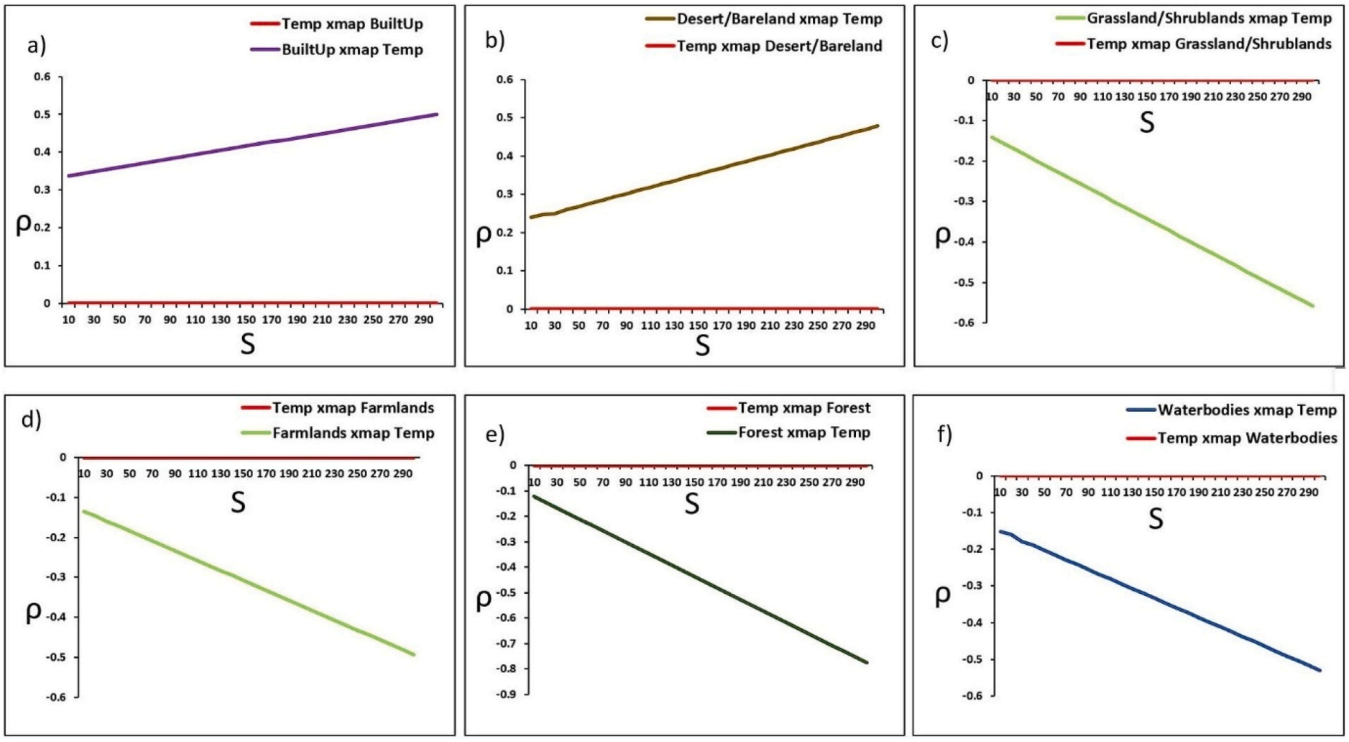

Fig. 10. GCCM Output of (a) Built Up and Temp; (b) Desert/Bareland and Temp; (c) Grassland/Shrubland and Temp; (d) Farmlands and Temp (e) Forests and Temp and (e) Waterbodies and Temp, s represents sample of points, and ρ depicts the Cross-mapping Skill values.

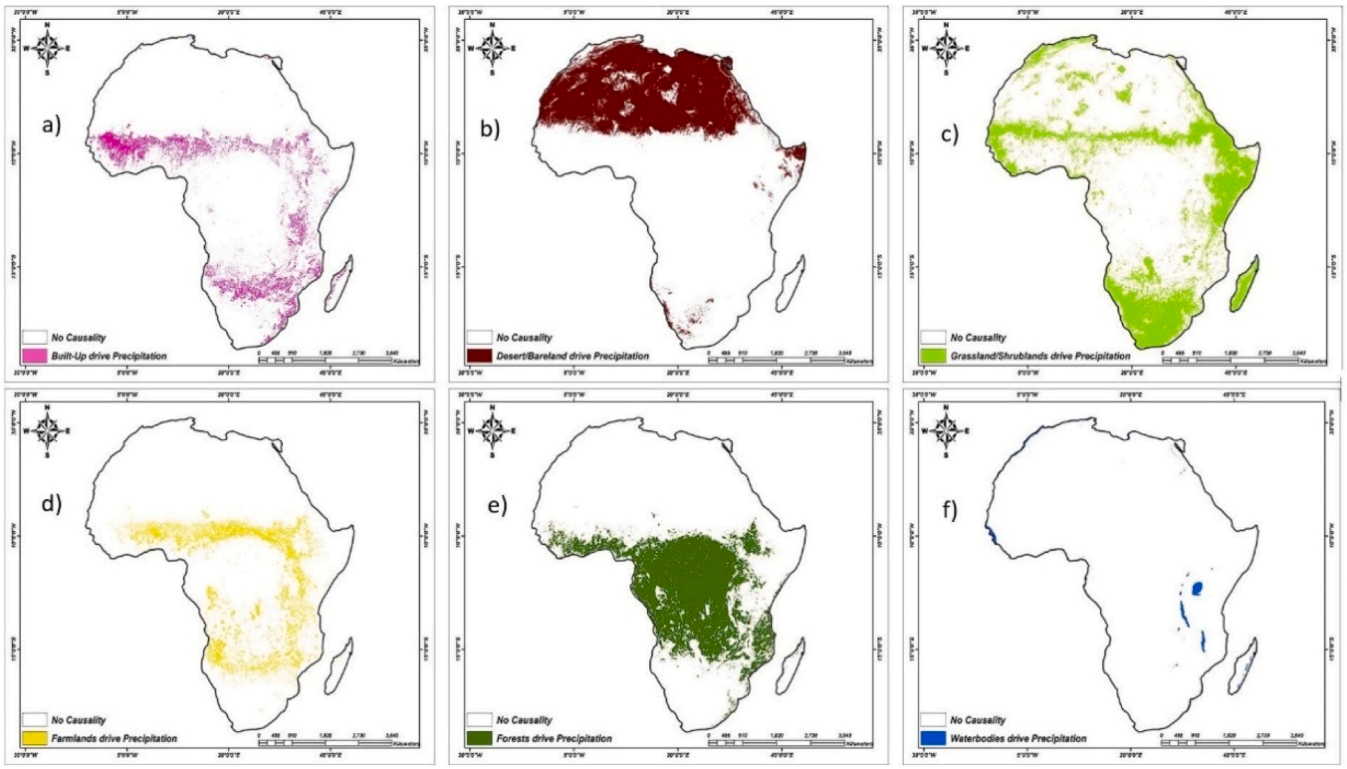

Fig. 11. GCCM Output of CCM outputs of (a) Built Up and Precip; (b) Desert/Bareland and Precip; (c) Grassland/Shrubland and Precip; (d) Farmlands and Precip (e) Forests and Precip and (e) Waterbodies and Precip and ρ depicts the Cross-mapping Skill values.

values between grasslands/shrublands and temperature, with ρ values starting near 0 and dropping to around −0.35 by time step 30. This negative correlation suggests that the presence of grasslands and shrublands is associated with lower temperatures, possibly due to the cooling effects of vegetation through processes like evapotranspiration and shading. However, the declining trend in ρ implies that the

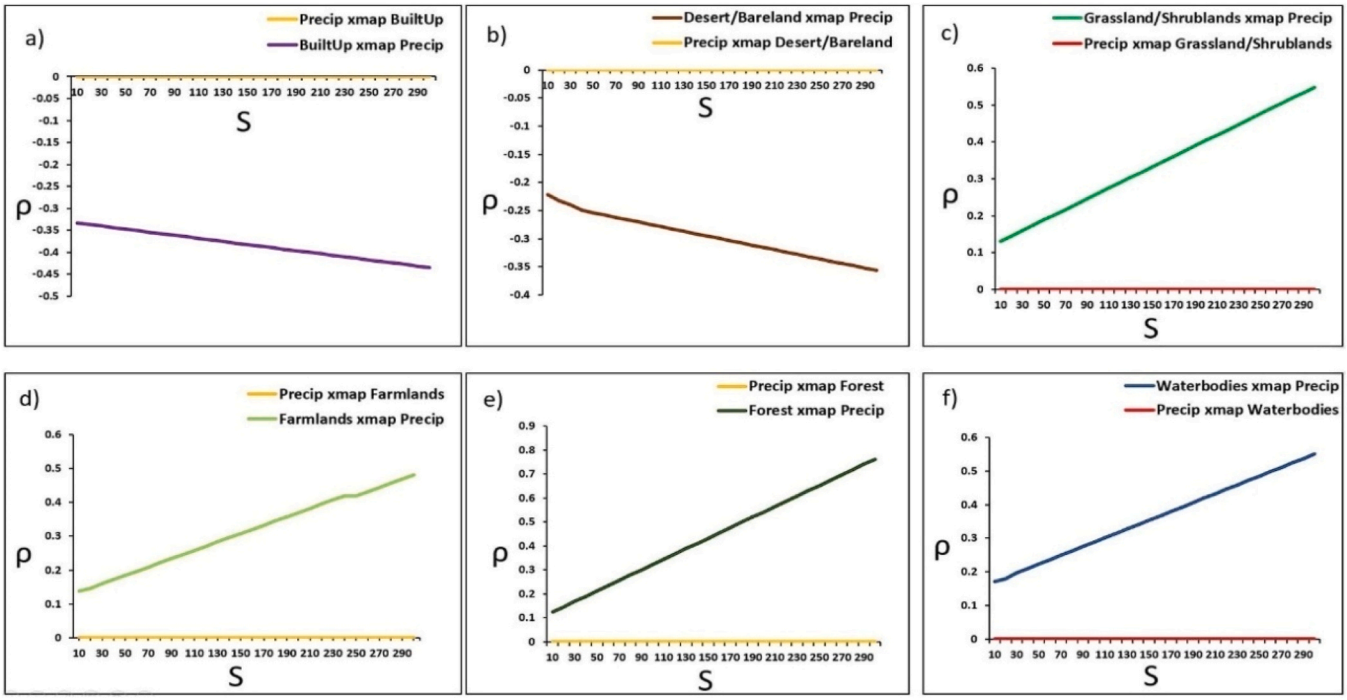

Fig. 12. GCCM Output of CCM outputs of (a) Built Up and Precip; (b) Desert/Bareland and Precip; (c) Grassland/Shrubland and Precip; (d) Farmlands and Precip (e) Forests and Precip and (e) Waterbodies and Precip, *s* represents sample of points and ρ depicts the Cross-mapping Skill values.

degradation or loss of grasslands/shrublands may lead to reduced cooling capacity, contributing to local temperature increases. This trend is concerning, as it indicates that ongoing degradation of these ecosystems could exacerbate warming, particularly in semi-arid and arid regions where grasslands are a dominant land cover. Farmlands, forests, and waterbodies exhibit negative cross-prediction skill values with temperature, with ρ values reaching around −0.55, −0.65, and −0.70 respectively by time step 30. These causations indicate that these land cover types have a cooling effect on local temperatures. Farmlands, through agricultural practices, can contribute to cooling via evapotranspiration and crop cover. Forests, with their dense vegetation, provide significant shading and cooling through transpiration, making them critical for temperature regulation. Waterbodies, with their high specific heat capacity, moderate local temperatures by absorbing heat during the day and releasing it slowly at night. The consistent negative causation over time emphasizes the importance of preserving and managing these land cover types to mitigate local temperature increases, especially in the context of climate change. This is particularly important in areas close to waterbodies given that Ghana currently is experiencing increasing sea level rise of 2.1 mm per year (Stark and Terasawa, 2013), directly impacting flooding occurrences.

3.6.2. *Temporal causal inference: precipitation and LULCC variables*

The CCM results in Fig. 8 reveal strong negative causation between built-up areas and precipitation, with ρ values decreasing from around −0.1 to nearly −0.8 by time step 30. This indicates that urbanization is associated with a significant reduction in precipitation. Urban areas, with their impervious surfaces, disrupt natural hydrological cycles, reducing moisture availability for precipitation through decreased infiltration and increased runoff. The sharp decline in ρ suggests that as cities expand, they contribute to drying trends, which could have severe implications for water availability and agricultural productivity. The strong inverse relationship highlights the need for green infrastructure and urban planning strategies that enhance water retention and mitigate the adverse effects of urbanization on precipitation. Desert/bare lands exhibit a negative correlation with precipitation, with ρ values decreasing to around −0.7 by time step 30. This indicates that the expansion of desert or bare land areas is associated with reduced precipitation, likely due to the lack of vegetation, which limits evapotranspiration and moisture availability. The strong negative trend underscores the feedback loop between land degradation and climate, where the expansion of deserts not only results from reduced precipitation but also contributes to its further decline. This highlights the urgent need for desertification control measures to break this cycle and restore land productivity.

Farmlands and forests both show positive correlations with precipitation, with ρ values reaching around 0.55 and 0.65 respectively by time step 30. These positive trends suggest that these land covers enhance local precipitation through moisture recycling and cloud formation. Forests, in particular, play a critical role in maintaining the hydrological cycle, and their preservation is essential for sustaining precipitation levels. Waterbodies also exhibit a strong positive correlation with precipitation, with ρ values increasing to around 0.65 by time step 30. Waterbodies contribute to local humidity and cloud formation, which can enhance precipitation. The positive correlations for farmlands, forests, and waterbodies highlight the importance of integrated land and water management strategies to sustain regional precipitation patterns in the face of climate change.

3.6.3. *Spatial causal inference: temperature and LULCC variables*

The spatial distribution of built-up areas driving temperature (Fig. 9a) shows a significant concentration of causality in urbanized regions, particularly in North and West Africa. The accompanying GCCM plot (Fig. 9a) displays a steadily increasing cross-mapping skill (ρ) over time, with ρ values reaching up to 0.55, indicating a strong causal relationship. This spatial pattern reflects the urban heat island (UHI) effect, where densely populated and industrialized areas experience higher temperatures due to reduced vegetation and increased anthropogenic activities. The map highlights that desert/bare land areas (Fig. 9b) are predominantly driving temperature increases in the Sahara region and parts of the Sahel. The corresponding GCCM plot shows a moderate causation, with ρ reaching approximately 0.6 (Fig. 10b). This suggests that desertification and the expansion of bare lands are critical contributors to rising temperatures in these regions, largely due to the

reduced albedo and diminished evapotranspiration.

For grasslands/shrublands (Fig. 9c), the GCCM results indicate a broader distribution of causality across central and southern Africa. The causation decreases over time (ρ trending negatively) (Fig. 10c), suggesting that these ecosystems have a cooling effect on temperature. However, the decreasing trend implies that as grasslands degrade, their ability to mitigate temperature rise diminishes, leading to localized warming. The GCCM analysis for farmlands, forests, and waterbodies (Fig. 9(d, e, f) and Fig. 10(d, e, f)) indicates that these land covers primarily drive temperature in regions with extensive agricultural activities (farmlands in yellow) and dense forest cover (dark green). The negative ρ values in the plots confirm that these land covers generally have a cooling effect on the local climate, particularly in areas like the Congo Basin and the Ethiopian Highlands. The strong negative correlations suggest that preserving these ecosystems is vital for maintaining cooler regional climates.

3.6.4. Spatial causal inference: precipitation and LULCC variables

The spatial GCCM map for built-up areas driving precipitation (Fig. 11a) shows causality concentrated in regions with rapid urbanization, particularly in West Africa. The corresponding GCCM plot reveals a declining ρ value (Fig. 12a), indicating that urbanization is associated with reduced precipitation. This decline reflects the disruption of natural hydrological cycles by impervious surfaces, leading to decreased infiltration and increased runoff. The desert/bare land GCCM map (Fig. 11b) highlights that these areas are driving reduced precipitation, particularly in the Sahara and Sahel regions. The negative trend in ρ (Fig. 12b) reflects the impact of desertification on precipitation, where the expansion of arid areas contributes to a feedback loop of declining moisture availability and further desertification.

The grasslands/shrublands GCCM map (Fig. 11c) indicates that these land cover types drive precipitation over large parts of the African continent, especially in central and southern regions. The positive cross-mapping prediction (ρ) (Fig. 12c) in the GCCM plot suggests that these ecosystems play a crucial role in maintaining precipitation levels. The spatial distribution aligns with the importance of these ecosystems in moisture recycling and cloud formation, essential for sustaining precipitation patterns. The GCCM results for farmlands, forests, and waterbodies (Fig. 11d, e and f) show that these land cover types drive precipitation in regions with extensive vegetation and water bodies. The positive ρ values (Fig. 12d, e and f) indicate that these ecosystems enhance local precipitation through mechanisms such as evapotranspiration and moisture recycling. The maps highlight the importance of these land covers in maintaining precipitation in regions like the Congo Basin and the Great Lakes area.

3.7. Future LULCC projections for Africa

The LULCC prediction for Africa, as illustrated in the maps for 2033, 2043, and 2053, shows significant transformations across the continent over the study period. The change detection statistics (Tables 4–6) for projected land-use trends in Africa (Fig. 13) suggest significant shifts in land cover classes between 2023 and 2053. Notably, built-up areas are expected to see a dramatic increase of 41.54 %, followed by waterbodies with an 15.59 % rise, farmlands expanding by 8.51 % and forests increasing by 1.51 %. These land cover types are anticipated to undergo substantial expansion during the study period. Conversely, desert/bare lands are predicted to decline sharply by 17.78 %, and grasslands/shrubs decreasing by 14.36 % (Table 5). Furthermore, the rate and magnitude (Table 6) of change analyses emphasize that built-up areas, waterbodies, farmlands and forests will grow at annual rates of 1.38 %, 0.52 %, 0.28 % and 0.05 %, respectively, progressively replacing other land cover types like grasslands and forests. This rapid transformation highlights the intensification of agricultural practices, urbanization, and desertification across the continent.

On the other hand, desert/bare lands and grasslands/shrubs are expected to experience significant annual reductions of 0.59 % and 0.48 %, respectively. The decline in these crucial ecosystems reflects the ongoing pressures of deforestation, land degradation, and the impact of climate change, leading to the loss of biodiversity and vital ecosystem services. These trends underscore the urgent need for sustainable land management practices to mitigate the adverse effects of these changes on Africa's environment and livelihoods.

Table 4
Area coverage (sq.km) for LULCC in Africa based on future projections (2023–2053).

Classes	2023	2033	2043	2053
Farmlands	3041,842	3425,871	3198,212	2970,553
Desert/Bareland	5168,974	4724,054	4487,016	4249,978
Built-Up	2531,036	2690,327	3136,432	3582,537
Grasslands/ Shrublands	4798,460	4734,531	4586,902	4439,274
Forests	14,304,287	14,302,161	14,411,255	14,520,349
Waterbodies	525,401	493,057	550,183	607,309

***Total area coverage (Km^2) (Absolute area) = 30,370,000.

Table 5
Land cover changes between the given study periods (%) (2023–2053).

Classes	2023–2033	2033–2043	2043–2053	2023–2053
Farmlands	+ 17.56	−3.85	−4.00	+ 8.51
Desert/Bareland	−8.61	−5.02	−5.28	−17.78
Built-Up	+ 6.29	+ 16.58	+ 14.22	+ 41.54
Grasslands/ Shrublands	−4.46	−5.18	−5.47	−14.36
Forests	−0.01	+ 0.76	+ 0.76	+ 1.51
Waterbodies	−6.16	+ 11.59	+ 10.38	+ 15.59

3.8. Future temperature projections for Africa

The temperature predictions for 2033, 2043, and 2053 reveal a consistent trend of rising temperatures across Africa, with significant variations across different regions. By 2053, the highest temperature range is expected to reach 36.88°C, with the lowest being around 8.87°C. The increase in temperature is most pronounced in the northern and central regions of Africa, where desert and semi-arid conditions prevail. This escalation in temperature aligns with the expanding desert/barren land cover, indicating a strong correlation between land cover changes and climate warming. The gradual increase in temperature over the decades underscores the ongoing impact of global climate change, which is likely to exacerbate the challenges of water scarcity, heat stress, and agricultural productivity in these regions.(Fig. 14)

3.9. Precipitation projections for Africa

The precipitation predictions for 2033, 2043, and 2053 show a declining trend in overall rainfall across the continent. By 2053, the maximum precipitation is projected to drop to 338.85 mm, down from 364.50 mm in 2033. The most significant reductions in precipitation are observed in the central and southern regions, where rainforests and grasslands are prevalent. This decline in rainfall is closely linked to the observed and predicted decreases in forest and grassland cover, highlighting the interdependence between land cover and precipitation patterns. The reduction in precipitation is likely to have severe implications for water availability, agriculture, and biodiversity, further stressing ecosystems already vulnerable to land use pressures.(Fig. 15)

3.10. Model performance and validation

The validation results indicate in Table 7 show a strong predictive performance across all models, with R^2 values ranging from 0.82 to 0.91, demonstrating a high correlation between observed and predicted

Table 6
Rate and magnitude of change (sq.km) of LULCC in Africa (2023–2053).

Classes	2023 (sq.km)	2053 (sq.km)	Magnitude of change (sq.km)	Magnitude of change (sq.km)/year	Annual Rate of change (%)
Farmlands	3041,842	2970,553	+ 258,711.10	+ 8624	+ 0.28
Desert/Bareland	5168,974	4249,978	−918,996.50	−30,633	−0.59
Built-Up	2531,036	3582,537	+ 1051,501.50	+ 35,050	+ 1.38
Grasslands/Shrublands	4798,460	4439,274	−689,186.40	−22,973	−0.48
Forests	14,304,287	14,520,349	+ 216,062.20	+ 7202	+ 0.05
Waterbodies	525,401	607,309	+ 81,907.80	+ 2730	+ 0.52

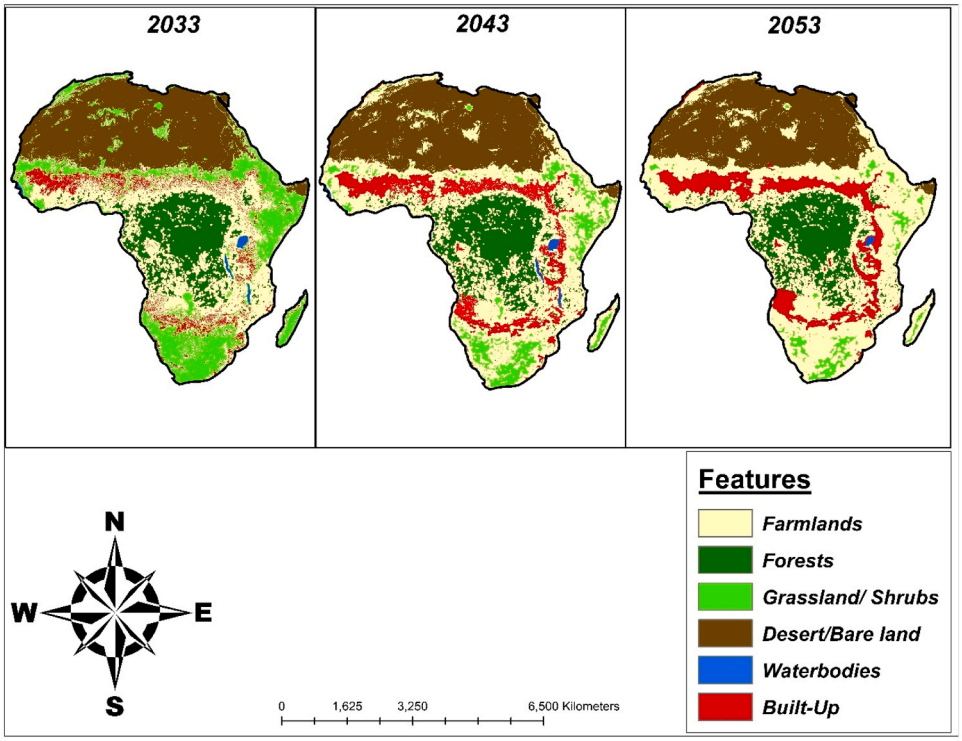

Fig. 13. Predicted land use and land cover trends in Africa.

climate variables. The Random Forest model achieved the highest accuracy for temperature predictions ($R^2 = 0.91$, RMSE = 1.12°C, MAE = 0.89°C), followed by the CCM-based model ($R^2 = 0.89$, RMSE = 1.27°C, MAE = 1.01°C). For precipitation, the Random Forest model also performed well ($R^2 = 0.85$, RMSE = 10.8 mm, MAE = 8.5 mm), indicating a reliable representation of precipitation variations. The ANN-CA model, though slightly less accurate than Random Forest, still exhibited strong performance, with R^2 values of 0.87 for temperature (RMSE = 1.35°C, MAE = 1.02°C) and 0.82 for precipitation (RMSE = 12.4 mm, MAE = 9.7 mm).

4. Discussion

4.1. Drivers of LULCC

Land use and land cover change in Africa has undergone significant transformations over the past decades, driven by urbanization, deforestation, and climate change. These processes have reshaped ecosystems, biodiversity, and regional climate patterns, creating environmental challenges across the continent. Urbanization has emerged as one of the leading drivers of LULCC, with rapid population growth and the expansion of cities leading to the conversion of natural landscapes into built-up areas. From 1980–2020, the built-up area in Africa increased by more than 80 %, particularly in nations like Nigeria, Ethiopia, and Ghana (United Nations, 2019). This urban expansion not only reduces natural vegetation cover but also contributes to environmental degradation, including soil erosion, pollution, and the urban heat island effect (Seto et al., 2012).

Desertification, particularly in the Sahel and North African regions, has also played a key role in shaping land cover changes. Overgrazing, unsustainable farming practices, and climate change have accelerated land degradation, leading to the spread of desert-like conditions in previously arable lands. The loss of vegetation cover, in turn, exacerbates land degradation, creating a feedback loop of declining productivity and food insecurity (Middleton and Thomas, 1997). Efforts to combat desertification, such as the Great Green Wall initiative, aim to restore degraded landscapes and halt the advance of deserts across the Sahel (Goffner et al., 2019). Climate change itself is both a driver and a result of LULCC in Africa. Rising temperatures, erratic rainfall, and extreme weather events have altered land use practices, forcing communities to expand agricultural lands or abandon degraded areas. In the Horn of Africa, recurrent droughts have led to increased land degradation, while LULCC has also contributed to global warming by reducing carbon storage and altering the reflectivity of the Earth's surface (Mutai et al., 2012; Pielke et al., 2011). To address these challenges, African countries have implemented sustainable land management policies, such as reforestation programs and conservation agriculture, which are essential for promoting environmental sustainability and resilience (UNEP, 2019).

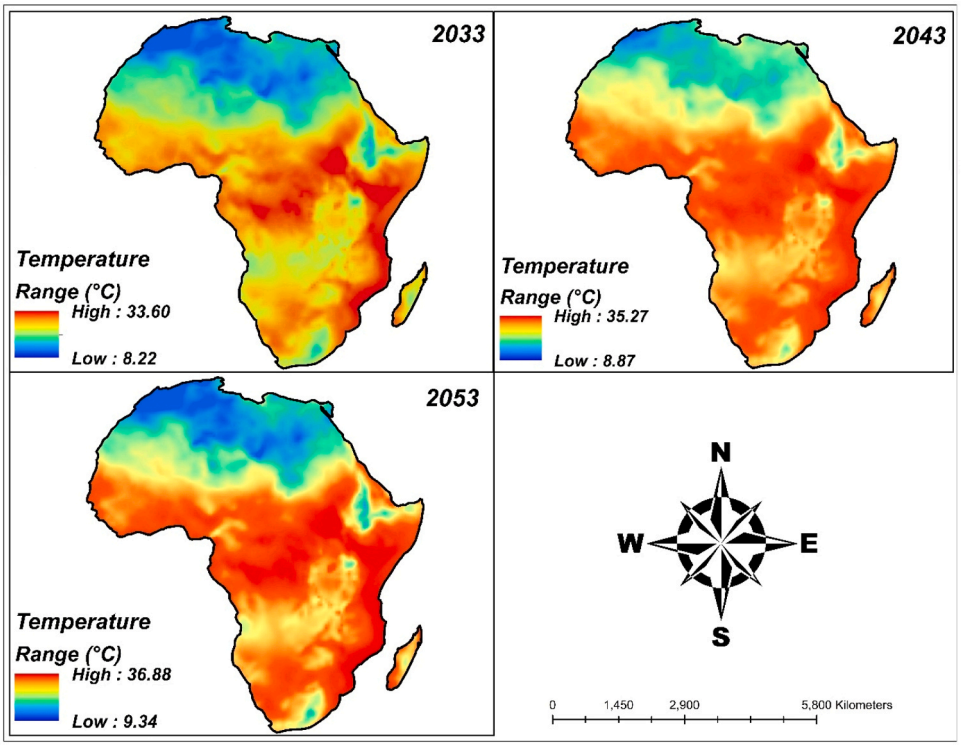

Fig. 14. Predicted Temperature trends in Africa.

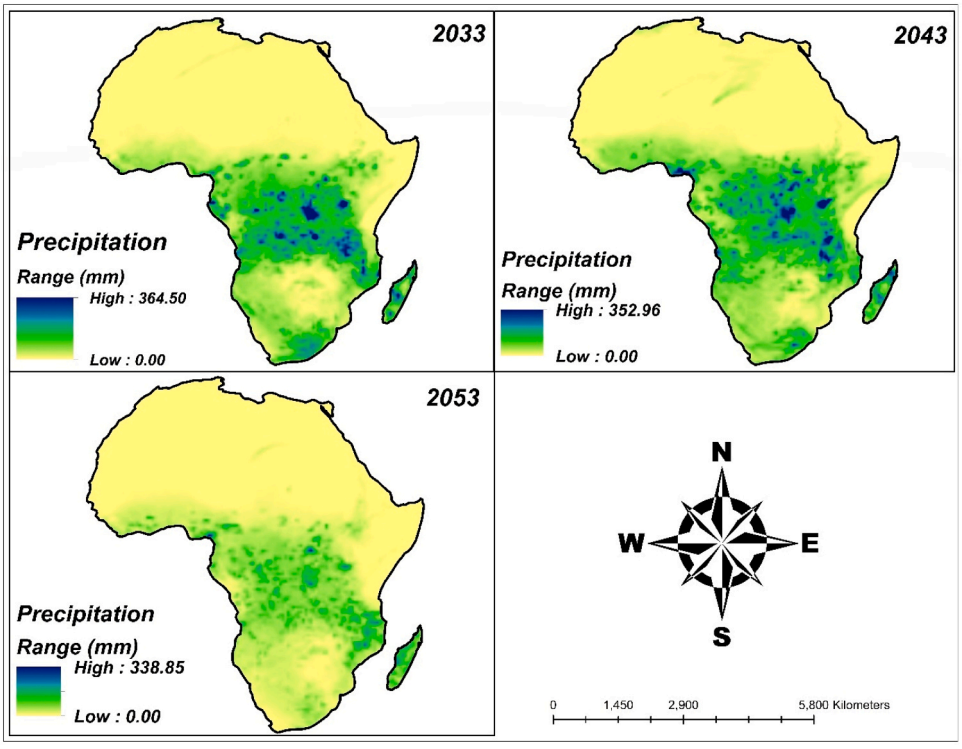

Fig. 15. Predicted Precipitation trends in Africa.

4.2. LULCC effects on temperature

LULCC significantly influences temperature patterns across Africa, particularly due to urbanization and deforestation. The rapid expansion of urban areas has led to the urban heat island (UHI) effect, where urban zones experience higher temperatures than rural areas due to the replacement of natural surfaces with concrete and buildings. In cities like Lagos, Accra, and Nairobi, studies have shown temperature differences of 2°C to 5°C between urban and rural areas, intensifying heatwaves and increasing energy demands (Makuma et al., 2020; Zhou et al., 2014). This localized warming can have serious health and environmental consequences. The predicted rise in temperatures and

Table 7
Quantitative Validation Metrics for Model Performance in Temperature and Precipitation Predictions Across Africa.

Model	Variable	R^2	RMSE (°C/mm)	MAE (°C/mm)
ANN-CA	LST (°C)	0.87	1.35	1.02
ANN-CA	Precipitation (mm)	0.82	12.4	9.7
RF	LST (°C)	0.91	1.12	0.89
RF	Precipitation (mm)	0.85	10.8	8.5
CCM-Based Model	LST (°C)	0.89	1.27	1.01
CCM-Based Model	Precipitation (mm)	0.83	11.6	9.1

subsequent heatwaves are likely to increase the incidence of health-related conditions such as heat exhaustion, heatstroke, dehydration and hyperthermia, particularly among vulnerable populations like the elderly, children, those with pre-existing health conditions and outdoor workers in densely built urban areas like Accra, Lagos and Cairo which experience urban heat island effect (Kwofie et al., 2022; Haines and Ebi, 2019; Watts et al., 2018). Specifically, studies in Accra (Wiru et al., 2020) and Lagos (Adelekan, 2020; Kunda et al., 2024) estimate about 9 % increase in heat-related mortality in Accra by 2050, and 10–15 % rise in heat-related deaths, particularly among vulnerable populations including the elderly and those with pre-existing health conditions in Lagos by 2060. Prolong exposure to high temperatures has also been shown to exacerbate cardiovascular and respiratory diseases, as heat places additional stress on the human body (Liu et al., 2024; Singh et al., 2024).

Furthermore, warmer temperatures and erratic rainfall can create ideal breeding conditions and extend the transmission period for vector-borne diseases, introducing these diseases into previously unaffected areas (Obame-Nkoghe et al., 2024; Colón-González et al., 2021). This can pose significant public health challenges, particularly in many communities in Africa which have limited healthcare infrastructure (Lucero-Prisno et al., 2022). Changing temperature and precipitation patterns in cities like Nairobi, Dar es Salaam and Kampala have significantly altered the distribution and activity of disease vectors, such as mosquitoes and ticks, increasing the risk of vector-borne diseases like malaria, dengue fever, and Zika virus (Tapia-Barredo et al., 2019). For instance, low-risk outskirts of Nairobi are estimated to experience about 20 % increase in malaria incidence by 2060 and in Dar es Salaam, cases of dangue are expected to surge by an estimated 40 % by 2080 due to an increase in the transmission period (Baharom et al., 2021). Deforestation is another major driver of temperature changes in Africa. The loss of forest cover, particularly in regions like the Congo Basin, reduces evapotranspiration and increases surface albedo, leading to higher local temperatures. As forests are replaced by impervious surfaces, the natural cooling effect provided by vegetation is diminished, exacerbating warming trends. This shift is evident in regions like West Africa, where large-scale deforestation has led to measurable increases in surface temperatures (Feddema et al., 2005; Malhi et al., 2008).

On a global scale, LULCC in Africa impacts the carbon cycle by reducing the amount of carbon sequestered by forests, which contributes to rising CO2 levels and global warming. As such, addressing LULCC through sustainable land-use practices, reforestation, and climate-resilient development strategies is essential for mitigating the long-term impacts of climate change on both local and global scales (Lawrence and Vandecar, 2015).

4.3. LULCC effects on precipitation

LULCC in Africa has a significant impact on precipitation patterns, altering both local and regional climates. Deforestation, particularly in areas like the Congo Basin and West Africa, disrupts the natural water cycle by reducing evapotranspiration. Forests play a critical role in releasing moisture into the atmosphere, which contributes to rainfall generation. When forests are cleared for agriculture or urbanization, the moisture input into the atmosphere decreases, leading to reduced local precipitation and potentially contributing to droughts (Lawrence and Vandecar, 2015; Makarieva et al., 2006). This shift in rainfall patterns has been observed in deforested regions, where the removal of trees leads to a decline in precipitation and longer dry spells. In addition to deforestation, the conversion of natural vegetation to cropland and urban areas can influence precipitation through changes in land surface properties such as albedo and surface roughness. Croplands generally have higher albedo than forests, meaning they reflect more sunlight, leading to reduced surface heating and weaker convection, which is necessary for cloud formation and rainfall. Urbanization, on the other hand, increases surface roughness and the heat island effect, which can cause localized changes in precipitation patterns, often leading to increased rainfall in and around urban areas due to enhanced convection (Shepherd, 2005). However, this can also lead to imbalanced precipitation, with urban areas receiving more rainfall at the expense of surrounding rural regions.

Numerous studies highlight the link between precipitation imbalances and health issues, particularly water-borne illnesses, food insecurity, and malnutrition. Increased rainfall and flooding in urban areas often contaminate water sources, resulting in a rise in diseases like cholera, typhoid fever, and diarrhea, especially in vulnerable African communities (Cisse et al., 2019; Levy et al., 2016). Floodwaters can transport pathogens into drinking supplies, exacerbating these health challenges, particularly where infrastructure is poor (Noor, 2023). Research in Southern and West Africa has shown a correlation between cholera outbreaks and flooding, impacting informal communities in Zambia (Kaseya et al., 2024) and Sierra Leone (Bangura et al., 2020). Conversely, droughts in cities like Cape Town limit access to clean water, forcing vulnerable populations to rely on unsafe water sources, further spreading water-borne diseases (Guppy et al., 2018). Moreover, changing precipitation patterns and high temperatures adversely affect agricultural productivity, contributing to food insecurity, increased food prices, and malnutrition in Africa, where many depend on rain-fed agriculture (Myers et al., 2017). This food insecurity has dire implications for child development, heightening the risks of malnutrition and related health issues (Tharumakunarajah et al., 2024).

The anticipated changes in temperature and precipitation across Africa have significant implications for several Sustainable Development Goals (SDGs), particularly Goal 3 (Good Health and Well-Being), Goal 2 (Zero Hunger), Goal 6 (Clean Water and Sanitation), and Goal 1 (No Poverty). Climate change poses a threat to achieving SDG 3 by increasing disease burden, limiting access to health services, and worsening health outcomes for vulnerable populations (Watts et al., 2018). Variable rainfall and rising temperatures disrupt food systems, complicating efforts to meet SDG 2 on food security (FAO, 2021). Additionally, water scarcity and contamination from climate change hinder progress towards SDG 6, crucial for reducing water-related diseases (Arora & Mishra, 2022). The health impacts of climate change can further entrench poverty by diminishing the capacity to work, thereby making it more challenging to achieve SDG 1 (Ebi et al., 2018). Thus, addressing these health issues through effective policies and climate resilience strategies is vital for Africa's sustainable development and for meeting the 2030 SDG targets.

The effects of LULCC on precipitation are not limited to local changes but can also extend to regional and continental scales through atmospheric circulation changes. Large-scale deforestation or land conversion can alter wind patterns and shift the position of major weather systems, such as the Intertropical Convergence Zone (ITCZ), which is responsible for much of the rainfall in sub-Saharan Africa. When land cover is changed extensively, the redistribution of heat and moisture can cause shifts in the ITCZ, leading to changes in seasonal precipitation

patterns across the continent (Devaraju et al., 2015). This disruption can lead to variability in rainy seasons, affecting agricultural productivity and water availability. LULCC in Africa significantly alters precipitation patterns through the modification of land surface characteristics, reduced evapotranspiration, and changes in atmospheric circulation. The implications are profound, particularly for regions reliant on consistent rainfall for agriculture and water resources. Addressing LULCC through reforestation, sustainable land management practices, and urban planning is essential to mitigate the negative effects on precipitation and ensure long-term climate resilience (Bonan, 2008; Taylor et al., 2002).

4.4. Policy implications: moving from science to decision-making

4.4.1. Integrating climate-resilient policies and projects into Africa's sub-regional development agenda

In recent years, the impact of climate change and its related stressors on the African continent has become increasingly evident. Rising temperatures (Fig. 4), prolonged droughts, and more frequent extreme weather events are threatening the livelihoods of millions of people. Therefore, it is imperative for African nations to integrate climate-resilient policies and projects into their development strategies to mitigate the effects of climate hazards and ensure sustainable growth. One of the key challenges these countries face is the lack of adequate infrastructure and resources to cope with climate change. Many African nations already struggle to provide basic services, such as clean water and sanitation, and the added pressure of climate change exacerbates these challenges. By incorporating climate-resilient policies and projects into their development plans, African nations can build more resilient infrastructure while also creating jobs and stimulating economic growth. Indicatively, they must adopt localized mitigation and adaptation mechanisms based on the principles of the 'grand urban model (GUM),' which emphasizes the development of sponge, garden, and low-carbon cities (Sarfo et al., 2023; Yeboah et al., 2025b). The 'Great Green Wall initiative,' for example, is a successful climate-resilient project that spans 11 nations in the Sahel and aims to combat desertification. This initiative has already planted millions of trees and created thousands of jobs for local communities. By integrating similar projects in other regions, African nations can protect their natural resources and improve the livelihoods of their people.

Oswald et al. (2020) utilized urban climate models and improved land use classifications to develop climate-resilient strategies in Klagenfurt, Austria. The findings from these studies underscore the need for a multifaceted approach to address climate-induced challenges. Such an integrated strategy combines various tools, policies, and methods that work together, aligning climate-resilient policies with urban heat mitigation efforts and ultimately fostering a more sustainable and livable society. The conclusions of these studies affirm the effectiveness of the 'causality approach' used in this research to evaluate the causal impact of changes in land use and cover on temperature and precipitation variations in Africa, along with their consequences. To effectively address climate risks and mitigation challenges, it is crucial to leverage emerging digital technologies, such as strategically placed ground-based temperature sensors across residential, commercial, and industrial areas to collect data on thermal variations. This data can then be analyzed and mapped using remote sensing technology, GIS, and various machine/-deep learning techniques. By employing these methodologies, we can identify, evaluate, and plan targeted interventions to address climate risks and extreme weather events, optimizing resources for maximum impact and enhancing the reliability of results from different approaches to mapping UHI (Elmarakby et al., 2022; Yeboah et al., 2025a).

Based on the analysis presented in Figs. 6–12, a key strategy that could be institutionalized across Africa's sub-regions is 'Leveraging Waterbodies for Urban Cooling.' Research by Liu et al. (2022), Zhi et al. (2018), and Gunawardena et al. (2017) highlights the crucial role waterbodies play in mitigating the adverse effects associated with climate hazards. Our findings are consistent with these studies, demonstrating that the cooling effects of water bodies can extend significantly, influencing the relationship between urban form factors and land surface temperature. Therefore, integrating urban hydrological processes, such as evaporative cooling, into climate-resilient policies and urban heat mitigation strategies can enhance efforts to reduce both land surface temperature (Fig. 4) and surface and near-surface UHI effects which are increasingly evident across Africa's sub-regions.

Optimizing 'green-blue infrastructure synergies' can improve the cooling effects of urban green and blue spaces in Africa's major cities. Integrating green features like parks and urban forests with water bodies such as rivers and lakes leads to greater temperature reductions than using either green or blue infrastructure alone. Projects like sustainable urban agriculture and other climate-friendly initiatives can further amplify cooling benefits, creating more comfortable microclimates for urban residents. According to Sarfo et al. (2023) and He et al. (2021), adaptation mechanisms based on the GUM principle aim to enhance community resilience against climate stressors through targeted measures for individuals, households, and populations. To effectively mitigate the negative impacts of climate disturbances, it is crucial to identify climate-induced hotspots and patterns, as well as the underlying driving forces in the region. This information forms the basis for developing local strategies to address these challenges.

Given the economically driven horizontal and vertical expansion of buildings and landscapes across Africa, implementing zero-UHI impact designs through green building initiatives and investing in renewable energy can help reduce LST and UHI intensity (Liu et al., 2022). This strategy includes measures such as using high-albedo materials, installing green roofs, and applying passive cooling techniques, which are essential for lowering thermal loads on buildings and enhancing climate resilience in African cities against extreme weather conditions. Furthermore, investing in climate-resilient infrastructure could stimulate local economies by creating green jobs and attracting eco-tourism. These infrastructure projects, combined with urban forests, parks, and recreational areas, not only increase property values but also contribute to the overall economic vitality of developing nations in Africa. Additionally, African nations could fulfill their commitments under the Paris Agreement and other international climate accords, potentially improving their access to funding and support from international organizations.

Community involvement and crowdsourcing through citizen science projects can greatly improve climate modeling and mitigation mapping efforts. Initiatives that encourage both rural and urban residents to report local temperatures and environmental conditions can enhance scientific data, leading to a more comprehensive understanding of large-scale climate events like sea level rise, increasing temperatures, coastal inundation and gradual submersion of land, prolonged dryness, and so on which affect vulnerable groups, resource-dependent communities, and coastal livelihoods/inhabitants. This, in turn, fosters community-driven solutions to mitigate the undesired consequences associated with extreme weather events or climate hazards. It is crucial to recognize that effective policies should be flexible and include monitoring and feedback mechanisms to address uncertainties and unintended consequences that may arise over time. These factors can significantly influence livability, thermal comfort, and resilience or sustainability efforts.

4.4.2. Need for adaptation justice amid land degradation, extreme weather conditions and sustainability concerns

This study examines the past, present, and future trends in Africa's land use, temperature, and precipitation. The predictions made based on prevailing trends are connected to the increasing demand for adaptation justice (AJ) (Lager et al., 2023; Juhola et al., 2022). Although various policy frameworks in Africa and some relevant works (Sarfo et al., 2024; Shi et al., 2016) have proposed adaptation strategies, they often fail to address the concerns of adaptation justice. In this study, we explored these concerns about land degradation and extreme weather conditions

in Africa. Juhola et al. (2022) and Shi et al. (2016) argue that 'adaptation justice' focuses on the fair distribution of resources, responsibilities, and opportunities as societies adapt to climate change and land degradation. This concept recognizes that vulnerable groups, such as those in Africa, often bear the brunt of climate stressors despite contributing the least to these phenomena. In this study, we emphasize the importance of incorporating adaptation justice into policy and theoretical frameworks that address land degradation and climate change concerns. Our goal is to ensure that no one is left behind in these efforts. We establish a clear connection between this innovative concept and specific Sustainable Development Goals (SDGs) such as poverty eradication (SDG 1), zero hunger (SDG 2), good health and well-being (SDG 3), access to quality

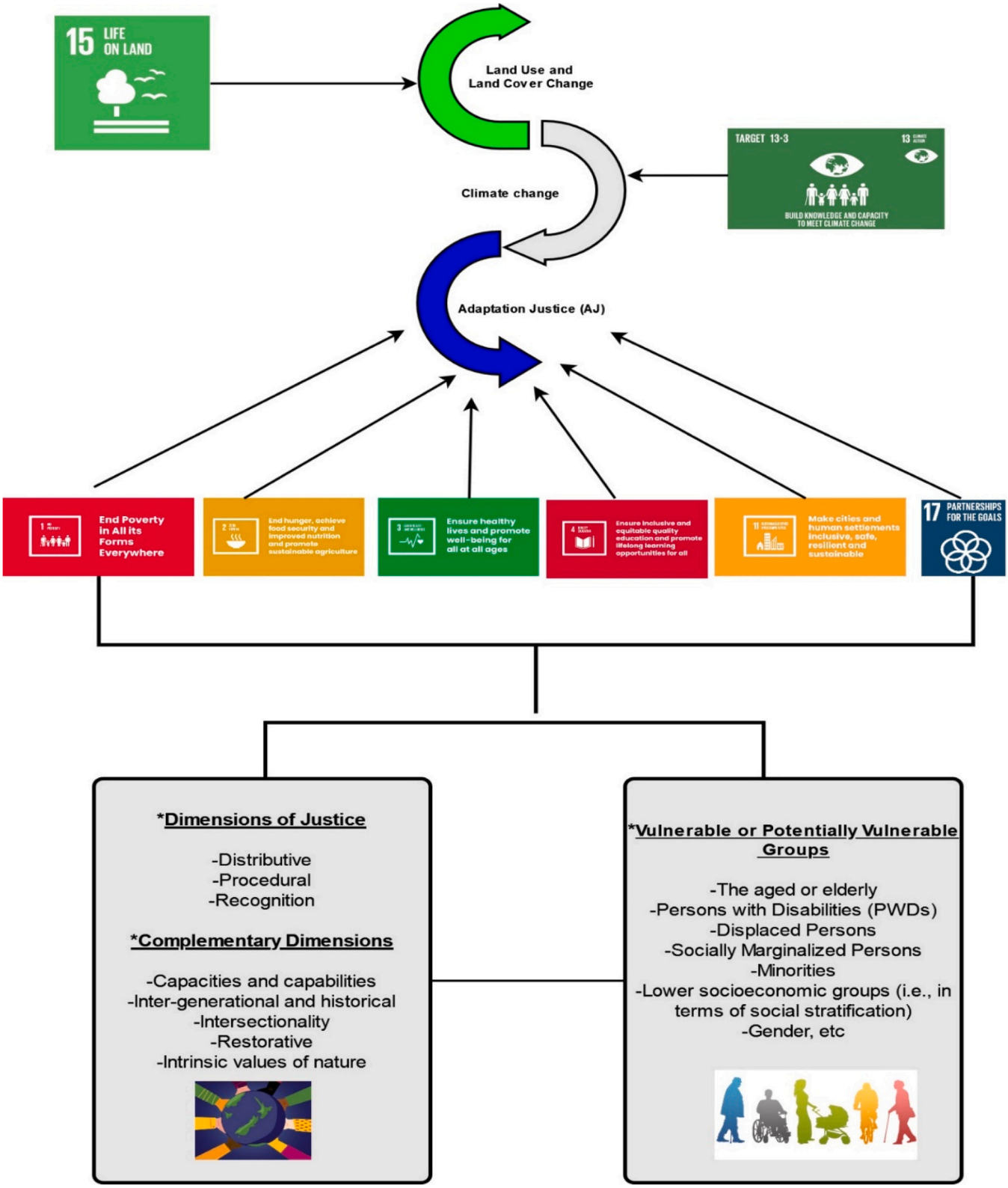

Fig. 16. Need for adaptation justice amid land degradation, extreme weather conditions and sustainability concerns.

education (SDG 4), sustainable cities and communities (SDG 11), climate action (SDG 13), life on land (SDG 15), and partnerships for inclusive development (SDG 17). By synergizing adaptation justice and these SDGs, we can create a fair and inclusive approach to addressing land degradation and climate hazards. This approach will reduce the burden on marginalized communities and prevent the exacerbation of existing inequalities in development efforts.

Based on the illustration mentioned earlier (Fig. 16), the dimensions of adaptation justice, which include distributive, procedural, and recognition, as stated in the IPCC (2022) sixth assessment report, aim to prevent climate hazards, land degradation, and adaptation measures from exacerbating poverty rates (SDG 1) in Africa. It is important to note that adaptation measures can lead to unintended consequences or maladaptation, so it is crucial to consider the potential impacts of planning and management. Vulnerable groups (Fig. 16) are often disproportionately affected by food insecurity, water scarcity, and climate-related disasters, and they often lack the resources to recover from these shocks. The emergence of community-led adaptation initiatives that empower local populations to build resilience is a key component of AJ processes. For example, the Community-Based Adaptation Program in Ethiopia (Capitani et al., 2018) has engaged communities in developing sustainable solutions to climate change impacts, such as implementing weather-resistant farming techniques and creating community-based early warning systems. These initiatives not only address the immediate impacts of climate change but also promote social justice by empowering marginalized populations to take charge of their own adaptation efforts. Therefore, this innovative concept emphasizes the need for adaptation policies, plans, programs, and projects (PPPPs) to prioritize and empower impoverished and vulnerable communities. This approach ensures that resources are distributed equitably and are accessible to enhance their adaptive capacity in both the short and long term. These principles are connected to the *'distributive dimension,'* which focuses on the benefits and burdens arising from land use, land cover change (LULCC), climate change impacts, and risks. The *'procedural dimension'* emphasizes the importance of clear pathways, meaningful participation, fairness, and legitimacy in adaptation processes. Lastly, the *'recognition dimension'* encompasses acknowledging diverse values and opinions while addressing underlying issues that contribute to distributive and procedural injustices in adaptation. Considering the principles and targets of SDG 2, which encompasses achieving 'Zero Hunger', it is crucial to recognize the close relationship between land degradation and climate hazards, as they directly impact agricultural productivity and food security. Unfortunately, marginalized communities are disproportionately affected by these issues. That is why AJ places a strong emphasis on creating resilient food systems that prioritize small-scale farmers and rural populations. These individuals are often the most vulnerable to climate disturbances and land degradation. In this context, we advocate for sustainable agricultural practices by promoting alternative green livelihoods and implementing agroforestry and precision agriculture techniques. Additionally, we aim to ensure access to climate-resilient crops and protect livelihoods that are dependent on food production.

Health inequalities, referred to as SDG 3, are often worsened by climate hazards. This includes extreme heat, water-borne diseases, and air pollution, which disproportionately affect low-income populations. The AJ concept emphasizes the importance of strengthening healthcare systems to increase the resilience of vulnerable groups against climate-related health risks, especially for those already facing barriers to healthcare access. To achieve this, the concept must address the underlying social determinants of health and promote equal access to clean air, water, and quality healthcare services. For example, the Solar for Health initiative in Tanzania provides solar-powered health facilities in remote areas, ensuring access to healthcare services even in the face of climate-related disruptions. By harnessing technological advancements and promoting innovation, these initiatives enhance resilience and promote justice in the face of climate change (Hunter et al., 2020). Similarly, SDG 4 focuses on education and effective communication about land degradation, climate change, and adaptation. In urban areas, for instance, successful AJ initiatives have been documented in cities like Douala, Lagos, and Accra, where local knowledge and resources have been leveraged to respond creatively to climate impacts (Williams et al., 2023; Filho et al., 2018). These actions often involve anticipatory and reactive measures by various actors, from individuals to international agencies. These studies report how the younger generations can be equipped with knowledge and skills to advocate for justice and innovation in scientific research. Lastly, both rural and urban areas, addressed by SDG 11, are highly susceptible to various climate events. These include flooding, urban heat island effects (UHIs), heat waves, and rising sea levels. Taking into consideration the social, economic, and cultural aspects of these phenomena, city planners, local and traditional authorities, international donors, and the scientific community in both rural and urban areas can integrate AJ when developing PPPPs for short, medium, and long-term sustainability. Sustainable policies in rural and urban areas should prioritize the needs of vulnerable communities through inclusivity (SDG 17) and resilient measures that prevent climate-induced displacement and protect the less fortunate. Through this concept, we advocate for strong global partnerships that go beyond adaptation mechanisms available only to nations or individuals with sufficient capacity to cope. Instead, these partnerships should provide equitable support to developing and susceptible regions, fostering shared responsibility and resources. Among the successful AJ scenarios in Africa is the regional collaboration among countries to address shared challenges. The African Union (AU) has played a critical role in fostering collaboration and cooperation among member states to tackle climate change impacts. For example, the African Risk Capacity (ARC) is a mutual insurance pool that helps member countries respond to climate-related disasters, providing financial support to vulnerable populations and ensuring a coordinated response to climate risks.

The concept of AJ is a fundamental principle within the framework of SDGs 13 and 15. AJ emphasizes the importance of not only technically effective mechanisms, but also socially just approaches. The aim is to cultivate empathy and ensure inclusivity in decision-making processes. In terms of inclusive decision-making processes, the Women's Climate Centers in Nigeria provide a platform for women to participate in climate-related decision-making processes, ensuring that their specific needs and vulnerabilities are taken into account (Filho et al., 2018). By incorporating diverse perspectives and promoting inclusivity, these initiatives foster equitable and just adaptation practices. In order to effectively address issues pertaining to land and climate hazards, it is crucial to distribute financial, technological, and technical support in a fair manner, taking into account the different responsibilities and capacities of nations and communities. For instance, the Green Climate Fund (GCF), provides financial support to African countries to implement climate adaptation projects that prioritize the needs of the most vulnerable populations. By mobilizing resources and ensuring that funding is allocated equitably, these initiatives promote climate justice by supporting those most affected by climate change (Hunter et al., 2020; Williams et al., 2023).

The impact of these under-researched phenomena extends beyond human activities to include other ecosystems and ecological processes. Consequently, communities or individuals who rely on these ecosystems for their livelihoods will remain at risk unless measures are taken to protect other ecosystems. Sustainable land management and conservation efforts must prioritize the rights and needs of indigenous communities in order to facilitate equitable and just adaptation strategies.

4.5. Limitations and future directions

While the use of remote sensing to assess the influence of LULCC on temperature and precipitation offers valuable insights, several limitations must be addressed. One key challenge lies in the trade-off between spatial and temporal resolution in satellite data, which can hinder the

accurate capture of both fine-scale land cover changes and short-term climatic variations. Additionally, remote sensing data often struggles to isolate the direct effects of LULCC from other atmospheric and human-induced factors, such as urbanization and industrialization, which can obscure the specific impacts on temperature and precipitation. The reliance on satellite data also introduces potential inaccuracies, particularly in regions like Africa, where ground-based validation is sparse. This can lead to misclassification of land cover types and inaccuracies in climate variable measurements. Moreover, the complexity of causal analysis methods, such as CCM, requires high-quality input data to establish reliable cause-and-effect relationships between LULCC and climate variables. The absence of consistent and reliable historical data in many African regions introduces significant uncertainties into the analysis.

Additionally, the diverse landscapes, microclimates, and socio-economic conditions across Africa present challenges to the generalization of the study's findings. The varying land cover types and climatic conditions throughout the continent influence the interactions between LULCC and climate in complex ways, meaning that the results of this broad-scale analysis may not fully capture the nuances of specific regions. As such, the findings may not be directly applicable to all regions without considering localized factors. Future research should focus on developing region-specific models that account for these regional differences, enabling more tailored and effective strategies for managing LULCC and its climatic impacts. By improving data quality, refining methodologies, and enhancing local-level analysis, future studies can address these limitations and provide more reliable insights into the dynamic relationship between land cover changes and climate systems across Africa.

5. Conclusions

In this study, we examined the causality between land use and land cover change (LULCC), and variations in temperature and precipitation across Africa. To do this, we employed integrated remote sensing techniques, causal inferences (i.e., Convergence Cross Mapping (CCM) and Geographical CCM), and representative studies. Additionally, we utilize Modules for Land Use Change Evaluation (MOLUSCE) and Artificial Neural Networks combined with Cellular Automata (ANN-CA) to simulate land use scenarios from 2033 to 2053. Our study draws the following conclusions based on the evidence gathered: (i) Our findings reveal a complex interplay of socio-political, economic, and biophysical factors influencing LULCC over the last three decades. During this period, northern and western Africa have experienced forest regrowth of + 2.61 %, alongside reductions in desert (-12.29 %), grassland/shrub (-14.20 %), and farmland (-14.53 %) coverage. In contrast, built-up areas expanded by + 134.63 %, and water bodies increased by + 71.63 %. (ii) Predicted trends suggest continued reductions in desert and bare land, with annual decreases of approximately 0.59 %, and declines of 0.48 % for grasslands and shrubs over the next 30 years. (iii) The analysis, supported by q-statistics, reveals significant correlations between LULCC and climatic variables. Rising temperatures in northern Africa are associated with desertification, while dense forests and water bodies in central and southern Africa help mitigate heat. (iv) K-means clustering identifies distinct regional patterns in the impacts of LULCC, underscoring the need for targeted interventions.

Our findings offer critical insights into the significant role that LULCC plays in altering local and regional climate patterns, particularly through processes such as urbanization, deforestation, and agricultural expansion. The application of causal inference models, such as CCM and GCCM, has enriched our understanding of these dynamics. As Africa continues to experience rapid land cover changes, the continent's unique environmental and socio-economic context presents both challenges and opportunities for climate impact studies. The insights from this research provide a foundation for policymakers and practitioners to design more targeted land-use policies and climate adaptation measures, helping to mitigate the adverse effects of LULCC on regional climate systems. Future research should focus on integrating more robust datasets, advancing methodological frameworks, and fostering interdisciplinary collaboration between remote sensing scientists, climatologists, and local policymakers. These efforts will be crucial in addressing the growing need for sustainable land management and climate adaptation strategies in the face of ongoing environmental changes.

Funding

This work is supported by the National Natural Science Foundation of China, No. 42401255, the 2024 Henan Provincial Postdoctoral Research Projects, No. HN2025109 and No. HN2025115 (J25001Y) and the General Project of Humanities and Social Sciences Research in Henan Higher Education Institutions (Project No: 2025-ZZJH-174).

CRediT authorship contribution statement

Sabastian Batasuma: Writing – review & editing. **Ebenezer Nikoi:** Writing – review & editing, Writing – original draft. **Isaac K. Arthur:** Writing – review & editing. **Owusu Alex Barimah:** Writing – review & editing. **Iris Ekua Mensimah Fynn:** Writing – review & editing. **Fareeha Siddique:** Writing – review & editing. **Isaac Sarfo:** Writing – review & editing, Writing – original draft, Visualization, Validation, Software, Investigation, Formal analysis, Conceptualization, Funding. **Rukhshinda Aftab:** Writing – review & editing. **Qiankun Zhu:** Writing – review & editing, Validation, Supervision, Investigation, Formal analysis, Funding. **Dinah Boyetey:** Writing – review & editing. **Clement Kwang:** Writing – review & editing, Formal analysis. **Williams Siaw:** Writing – review & editing. **Dzifa Adimle Puplampu:** Writing – review & editing, Writing – original draft. **Charafa El Rhadiouini:** Writing – review & editing. **Abraham Okrah:** Writing – review & editing. **Ali Hasan Jaffry:** Writing – review & editing. **Emmanuel Yeboah:** Writing – original draft, Visualization, Validation, Software, Resources, Methodology, Investigation, Formal analysis, Data curation, Conceptualization.

Declaration of Competing Interest

The authors declare that they have no known competing financial interests or personal relationships that could have appeared to influence the work reported in this paper.

Acknowledgement

The authors will like to thank the handling editor and anonymous reviewers for their insightful comments on the manuscript.

Appendix A. Supporting information

Supplementary data associated with this article can be found in the online version at doi:10.1016/j.landusepol.2025.107680.

Data availability

Data will be made available on request.

References

Abbasian, M., Moghim, S., Abrishamchi, A., 2019. Performance of the general circulation models in simulating temperature and precipitation over Iran. Theor. Appl. Climatol. 135, 1465–1483.

Achugbu, I.C., Olufayo, A.A., Balogun, I.A., Adefisan, E.A., Dudhia, J., Naabil, E., 2021. Modeling the spatiotemporal response of dew point temperature, air temperature and rainfall to land use land cover change over West Africa. Model. Earth Syst. Environ. 1–26.

Adelekan, Ibidun O., 2020. "Urban dynamics, everyday hazards and disaster risks in Ibadan, Nigeria. Environ. Urban. 32 (1), 213–232.

Akpoti, K., Antwi, E.O., Kabo-bah, A.T., 2016. Impacts of rainfall variability, land use and land cover change on stream flow of the black Volta Basin. In: West Africa, 3. Hydrology, p. 26.
Arora, N.K., Mishra, I., 2022. Sustainable development goal 6: global water security. Environ. Sustain. 5 (3), 271–275.
Baharom, M., Ahmad, N., Hod, R., Arsad, F.S., Tangang, F., 2021. The impact of meteorological factors on communicable disease incidence and its projection: a systematic review. Int. J. Environ. Res. Public Health 18 (21), 11117.
Bangura, J.B., Xiao, S., Qiu, D., Ouyang, F., Chen, L., 2020. Barriers to childhood immunization in sub-Saharan Africa: a systematic review. BMC Public Health 20, 1–15.
Bonan, G.B., 2008. Forests and climate change: Forcings, feedbacks, and the climate benefits of forests. Science 320 (5882), 1444–1449.
Burakowski, E., Tawfik, A., Ouimette, A., Lepine, L., Novick, K., Ollinger, S., Bonan, G., 2018. The role of surface roughness, albedo, and Bowen ratio on ecosystem energy balance in the Eastern United States. Agric. For. Meteorol. 249, 367–376.
Capitani, C., Garedew, W., Mitiku, A., Berecha, G., Hailu, B., Heiskanen, J., Hurskainen, P., Platts, P., Siljander, M., Pinard, F., Johansson, T., Marchant, R., 2018. Views from two mountains: exploring climate change impacts on traditional farming communities of Eastern Africa highlands through participatory scenarios. Sustain. Sci. 14, 191–203. https://doi.org/10.1007/s11625-018-0622-x.
Charney, J.G., 1975. Dynamics of deserts and drought in the Sahel. Q. J. R. Meteorol. Soc. 101 (428), 193–202.
Chen, L., Dirmeyer, P.A., 2016. Adapting observationally based metrics of biogeophysical feedbacks from land cover/land use change to climate modeling. Environ. Res. Lett. 11 (3), 034002.
Cisse, F.A., Damien, C., Bah, A.K., Touré, M.L., Barry, M., Djibo Hamani, A.B., Naeije, G., 2019. Minimal setting stroke unit in a sub-Saharan African public hospital. Front. Neurol. 10, 856.
Coll, C., Galve, J.M., Sanchez, J.M., Caselles, V., 2009. Validation of Landsat-7/ETM+ thermal-band calibration and atmospheric correction with ground-based measurements. IEEE Trans. Geosci. Remote Sens. 48 (1), 547–555.
Colón-González, F.J., Sewe, M.O., Tompkins, A.M., Sjödin, H., Casallas, A., Rocklöv, J., Lowe, R., 2021. Projecting the risk of mosquito-borne diseases in a warmer and more populated world: a multi-model, multi-scenario intercomparison modelling study. Lancet Planet. Health 5 (7), e404–e414.
Crétat, J., Vizy, E.K., Cook, K.H., 2014. How well are daily intense rainfall events captured by current climate models over Africa? Clim. Dyn. 42, 2691–2711.
Devaraju, N., Bala, G., Caldeira, K., 2015. Deforestation-induced climate change reduces future rainfall in the Amazon. Nat. Clim. Change 5 (4), 27–32.
Ebi, K.L., Hasegawa, T., Hayes, K., Monaghan, A., Paz, S., Berry, P., 2018. Health risks of warming of 1.5C, 2C, and higher, above pre-industrial temperatures. Environ. Res. Lett. 13 (6), 063007.
Elmarakby, E., Khalifa, M., Elshater, A., Afifi, S., 2022. Tailored methods for mapping urban heat islands in Greater Cairo Region. Ain Shams Eng. J. 13 (2), 101545. https://doi.org/10.1016/j.asej.2021.06.030.
Eriksen, S., Schipper, E.L.F., Scoville-Simonds, M., Vincent, K., Adam, H.N., Brooks, N., West, J.J., 2021. Adaptation interventions and their effect on vulnerability in developing countries: Help, hindrance or irrelevance? World Dev. 141, 105383.
FAO, 2021. The State of Food Security and Nutrition in the World 2021. Food and Agriculture Organization of the United Nations.
Feddema, J.J., Oleson, K.W., Bonan, G.B., Mearns, L.O., Washington, W.M., Meehl, G.A., Nychka, D., 2005. The importance of land-cover change in simulating future climates. Science 310 (5754), 1674–1678.
Filho, W., Balogun, A., Ayal, D., Bethurem, M., Murambadoro, M., Mambo, J., Taddese, H., Tefera, G., Nagy, G., Fudjumdjum, H., Mugabe, P., 2018. Strengthening climate change adaptation capacity in Africa- case studies from six major African cities and policy implications. Environ. Sci. Policy. https://doi.org/10.1016/J.ENVSCI.2018.05.004.
Foley, J.A., Ramankutty, N., Brauman, K.A., Cassidy, E.S., Gerber, J.S., Johnston, M., Zaks, D.P., 2011. Solutions for a cultivated planet. Nature 478 (7369), 337–342.
Glotfelty, T., Ramírez-Mejía, D., Bowden, J., Ghilardi, A., West, J.J., 2021. Limitations of WRF land surface models for simulating land use and land cover change in Sub-Saharan Africa and development of an improved model (CLM-AF v. 1.0). Geosci. Model Dev. 14 (6), 3215–3249.
Goffner, D., Sinare, H., Gordon, L.J., 2019. The Great Green Wall for the Sahara and the Sahel Initiative as an adaptation to climate change and desertification. Reg. Environ. Change 19 (5), 1417–1428.
Gunawardena, K.R., Wells, M.J., Kershaw, T., 2017. Utilising green and bluespace to mitigate urban heat island intensity. Sci. Total Environ. 584, 1040–1055.
Guppy, L., Uyttendaele, P., Villholth, K.G., & Smakhtin, V.U. (2018). Groundwater and sustainable development goals: Analysis of interlinkages.
Haines, A., Ebi, K., 2019. The imperative for climate action to protect health. N. Engl. J. Med. 380 (3), 263–273.
Houghton, R.A., House, J.I., Pongratz, J., Van Der Werf, G.R., Defries, R.S., Hansen, M.C., Ramankutty, N., 2012. Carbon emissions from land use and land-cover change. Biogeosciences 9 (12), 5125–5142.
Hulme, M., 1994. Validation of large-scale precipitation fields in general circulation models. In Global precipitations and climate change. Springer Berlin Heidelberg, pp. 387–405.
Hunter, N., North, M., Roberts, D., Slotow, R., 2020. A systematic map of responses to climate impacts in urban Africa. Environ. Res. Lett. 15. https://doi.org/10.1088/1748-9326/ab9d00.
IPCC. (2021). Climate Change 2021: The Physical Science Basis. Contribution of Working Group I to the Sixth Assessment Report of the Intergovernmental Panel on Climate Change.
IPCC, 2022. Climate Change 2022: Impacts, Adaptation and Vulnerability. Contribution of Working Group II to the Sixth Assessment Report of the Intergovernmental Panel on Climate Change. Cambridge University Press, Cambridge, UK and New York, NY, USA.
James, R., Washington, R., 2013. Changes in African temperature and precipitation associated with degrees of global warming. Clim. Change 117, 859–872.
Juhola, S., Heikkinen, M., Pietilä, T., Groundstroem, F., Käyhkö, J., 2022. Connecting climate justice and adaptation planning: An adaptation justice index. Environ. Sci. Policy 136, 609–619. https://doi.org/10.1016/j.envsci.2022.07.024.
Kaseya, J., Dereje, N., Tajudeen, R., Ngongo, A.N., Ndembi, N., Fallah, M.P., 2024. Climate change and malaria, dengue and cholera outbreaks in Africa: a call for concerted actions. BMJ Glob. Health 9 (3), e015370.
Kidane, Y., Stahlmann, R., Beierkuhnlein, C., 2012. Vegetation dynamics, and land use and land cover change in the Bale Mountains, Ethiopia. Environ. Monit. Assess. 184, 7473–7489.
Klein, C., Bliefernicht, J., Heinzeller, D., Gessner, U., Klein, I., Kunstmann, H., 2017. Feedback of observed interannual vegetation change: A regional climate model analysis for the West African monsoon. Clim. Dyn. 48, 2837–2858.
Kunda, J.J., Gosling, S.N., Foody, G.M., 2024. The effects of extreme heat on human health in tropical africa. Int. J. Biometeorol. 68 (6), 1015–1033.
Kwofie, S., Nyamekye, C., Appiah Boamah, L., Owusu Adjei, F., Arthur, R., Agyapong, E., 2022. Urban growth nexus to land surface temperature in Ghana. Cogent Eng. 9 (1), 2143045.
Lager, F., Coninx, I., Breil, M., Bakhtaoui, I., Branth Pedersen, A., Mattern, K., et al (2023). Just Resilience for Europe: Towards measuring justice in climate change adaptation. ETC CA. https://doi.org/10.25424/CMCC-BATP-3M95.
Lawrence, D., Vandecar, K., 2015. Effects of tropical deforestation on climate and agriculture. Nat. Clim. Change 5 (1), 27–36.
Levy, K., Woster, A.P., Goldstein, R.S., Carlton, E.J., 2016. Untangling the impacts of climate change on waterborne diseases: a systematic review of relationships between diarrheal diseases and temperature, rainfall, flooding, and drought. Environ. Sci. Technol. 50 (10), 4905–4922.
Li, X., Stringer, L.C., Dallimer, M., 2022. The impacts of urbanisation and climate change on the urban thermal environment in Africa. Climate 10 (11), 164.
Liu, X., Ming, Y., Liu, Y., Yue, W., Han, G., 2022. Influences of landform and urban form factors on urban heat island: Comparative case study between Chengdu and Chongqing. Sci. Total Environ. 820, 153395. https://doi.org/10.1016/j.scitotenv.2022.153395.
Liu, J., Qi, J., Yin, P., Liu, W., He, C., Gao, Y., Zhou, M., 2024. Rising cause-specific mortality risk and burden of compound heatwaves amid climate change. Nat. Clim. Change 14 (11), 1201–1209.
Lucero-Prisno, D.E.I., Kouwenhoven, M.B.N., Adebisi, Y.A., Miranda, A.V., Gyeltshen, D., Suleman, M.H., Wong, M.C., 2022. Top ten public health challenges to track in 2022. Public Health Chall. 1 (3), e21.
Makarieva, A.M., Gorshkov, V.G., Li, B.L., 2006. Conservation of water cycle on land via restoration of natural closed-canopy forests: implications for regional landscape planning. Ecol. Res. 21, 897–906.
Makuma, M.H., Gumbo, L., Mhangara, P., 2020. The impact of land use land cover changes on land surface temperature: A case study of Nairobi. Kenya Remote Sens. Appl. Soc. Environ. 18, 100305.
Malhi, Y., Roberts, J.T., Betts, R.A., Killeen, T.J., Li, W., Nobre, C.A., 2008. Climate change, deforestation, and the fate of the Amazon. Science 319 (5860), 169–172.
Marchant, R., Richer, S., Boles, O., Capitani, C., Courtney-Mustaphi, C.J., Lane, P., Wright, D., 2018. Drivers and trajectories of land cover change in East Africa: Human and environmental interactions from 6000 years ago to present. EarthSci. Rev. 178, 322–378.
Middleton, N., & Thomas, D. (1997). World atlas of desertification. United Nations Environment Programme.
Mishra, R.K., Upadhyay, S.K., 2022. Bayes analysis of abridged age specific fertility pattern using parametric models. Commun. Stat.-Theory Methods 51 (16), 5505–5533.
Moore, N., Andresen, J., Lofgren, B., Pijanowski, B., Kim, D.Y., 2015. Projected land-cover change effects on East African rainfall under climate change. Int. J. Climatol. 8, 1772–1783.
Mutai, C., et al., 2012. Climate variability and change in the Greater Horn of Africa: Impacts and adaptation options. Environmental. Development 5, 125–144.
Myers, S.S., Smith, M.R., Guth, S., Golden, C.D., Vaitla, B., Mueller, N.D., Huybers, P., 2017. Climate change and global food systems: potential impacts on food security and undernutrition. Annu. Rev. Public Health 38 (1), 259–277.
Noor, Afifa. "Effect of environmental seasons in the epidemiology of waterborne diseases: a review." PhD diss., Brac University, 2023.
Obame-Nkoghe, J., Agossou, A.E., Mboowa, G., Kamgang, B., Caminade, C., Duke, D.C., Otomo, P.V., 2024. Climate-influenced vector-borne diseases in Africa: a call to empower the next generation of African researchers for sustainable solutions. Infect. Dis. Poverty 13 (02), 83–92.
Oduro, C., Shuoben, B., Ayugi, B., Beibei, L., Babaousmail, H., Sarfo, I., Ngoma, H., 2022. Observed and Coupled Model Intercomparison Project 6 multimodel simulated changes in near-surface temperature properties over Ghana during the 20th century. Int. J. Climatol. 42 (7), 3681–3701.
Oduro, C., Lim Kam Sian, K.T.C., Hagan, D.F.T., Babaousmail, H., Ayugi, B.O., Wu, Y., Wu, N., 2025. The influence of land surface temperature on Ghana's climate variability and implications for sustainable development. Sci. Rep. 15 (1), 2595.
Oswald, S.M., Hollosi, B., Žuvela-Aloise, M., See, L., Guggenberger, S., Hafner, W., Prokop, G., Storch, A., Schieder, W., 2020. Using urban climate modelling and improved land use classifications to support climate change adaptation in urban

environments: A case study for the city of Klagenfurt, Austria. Urban Clim. 31, 100582. https://doi.org/10.1016/j.uclim.2020.100582.
Pielke, R.A., et al., 2011. Land use/land cover changes and climate: Modeling analysis and observational evidence. Wiley Interdiscip. Rev. Clim. Change 2 (6), 828–850.
Pieterse, E., Parnell, S., 2014. Africa's urban revolution in context. Afr. 'S. Urban Revolut. 1–17.
Rigden, A.J., Li, D., 2017. Attribution of surface temperature anomalies induced by land use and land cover changes. Geophys. Res. Lett. 44 (13), 6814–6822.
Sarfo, I., Bi, S., Xu, X., Yeboah, E., Kwang, C., Batame, M., Koku, J.E., 2023. Planning for cooler cities in Ghana: Contribution of green infrastructure to urban heat mitigation in Kumasi Metropolis. Land Use Policy 133, 106842.
Sarfo, I., Qiao, J., Yeboah, E., Puplampu, D.A., Kwang, C., Fynn, I.E.M., Sarfo, B.A., 2024. Meta-analysis of land use systems development in Africa: Trajectories, implications, adaptive capacity, and future dynamics. Land Use Policy 144, 107261.
Seto, K.C., Güneralp, B., Hutyra, L.R., 2012. Global forecasts of urban expansion to 2030 and direct impacts on biodiversity and carbon pools. Proc. Natl. Acad. Sci. 109 (40), 16083–16088.
Shepherd, J.M., 2005. A review of current investigations of urban-induced rainfall and recommendations for the future. Earth Interact. 9 (12), 1–27.
Shi, L., Chu, E., Anguelovski, I., et al., 2016. Roadmap towards justice in urban climate adaptation research. Nat. Clim. Change 6, 131–137. https://doi.org/10.1038/nclimate2841.
Singh, N., Areal, A.T., Breitner, S., Zhang, S., Agewall, S., Schikowski, T., Schneider, A., 2024. Heat and cardiovascular mortality: an epidemiological perspective. Circ. Res. 134 (9), 1098–1112.
Stark, J., Terasawa, K., 2013. Climate change and conflict in West African cities: a policy brief on findings from Lagos, Nigeria And Accra. US Agency for International Development, Ghana. Washington.
Swan, A., 2012. Policy guidelines for the development and promotion of open access. UNESCO Publishing.
Tapia-Barredo, L., Arredondo-Abreu, C.A., Ruiz-Matuk, C.B., & Paulino-Ramírez, R. (2019). Malaria: bad air— Is climate a reliable predictor for malaria case distributions in the Dominican Republic?. Transactions of the Royal Society of Tropical Medicine and Hygiene.
Taylor, C.M., Lambin, E.F., Stephenne, N., Harding, R.J., Essery, R.L., 2002. The influence of land use change on climate in the Sahel. J. Clim. 15 (24), 3615–3629.
Tharumakunarajah, R., Lee, A., Hawcutt, D.B., Harman, N.L., Sinha, I.P., 2024. The Impact of Malnutrition on the Developing Lung and Long-Term Lung Health: A Narrative Review of Global Literature. Pulm. Ther. 1–16.
UNEP, 2019. African Environmental Outlook 3: Summary for Policy Makers. United Nations Environment Programme.
UN-Habitat (2022) World cities report 2022: envisaging the future of cities. United Nations Research Institute for Social Development.
United Nations, 2019. World urbanization prospects: The 2018 revision. United Nations Department of Economic and Social Affairs.
Wang, X., Guo, W., Qiu, B., Liu, Y., Sun, J., Ding, A., 2017. Quantifying the contribution of land use change to surface temperature in the lower reaches of the Yangtze River. Atmos. Chem. Phys. 17 (8), 4989–4996.
Watts, N., Amann, M., Arnell, N., Ayeb-Karlsson, S., Belesova, K., Berry, H., Costello, A., 2018. The 2018 report of the Lancet Countdown on health and climate change: shaping the health of nations for centuries to come. Lancet 392 (10163), 2479–2514.
Williams, J., Chin-Yee, S., Maslin, M., Barnsley, J., Costello, A., Lang, J., Mcglade, J., Mulugetta, Y., Taylor, R., Winning, M., Parikh, P., 2023. Africa and climate justice at COP27 and beyond: impacts and solutions through an interdisciplinary lens. UCL Open Environ. 5. https://doi.org/10.14324/111.444/ucloe.000062.
Wiru, K., Oppong, F.B., Agyei, O., Zandoh, C., Nettey, O.E., Adda, R., Asante, K.P., 2020. The Influence of Apparent Temperature on Mortality in the Kintampo Health and Demographic Surveillance Area in the Middle Belt of Ghana: A Retrospective Time-Series Analysis. J. Environ. Public Health 2020 (1), 5980313.
Xiao, J., et al., 2022. Assessing the impacts of land use and land cover change on climate variability using remote sensing and modeling approaches. Remote Sens. 14 (1), 134.
Yan, D., Liu, T., Dong, W., Liao, X., Luo, S., Wu, K., Wen, X., 2020. Integrating remote sensing data with WRF model for improved 2-m temperature and humidity simulations in China. Dyn. Atmospheres Oceans 89, 101127.
Yeboah, E., Sarfo, I., Kwang, C., Alimo, P.K., Djan, M.A., Afenya, M.S., Okrah, A., Amankwah, S.O.Y., 2025a. Influence of land use patterns on urban heat island dynamics in an emerging megacity: A case study of Zhengzhou, Henan, China. J. Chin. Archit. Urban. 8412. https://doi.org/10.36922/jcau.8412.
Yeboah, E., Wang, G., Hagan, D.F.T., Shi, X., Cabral, P., Sarfo, I., Okrah, A., 2025b. A causal investigation of land use and land cover change on emerging urban heat island footprints in a mid-latitude region. Environ. Dev. Sustain. 1–34.
Yonaba, R., Mounirou, L.A., Tazen, F., Koïta, M., Biaou, A.C., Zouré, C.O., Yacouba, H., 2023. Future climate or land use? Attribution of changes in surface runoff in a typical Sahelian landscape. Comptes Rendus. Géoscience 355 (S1), 411–438.
Yosef, G., Walko, R., Avisar, R., Tatarinov, F., Rotenberg, E., Yakir, D., 2018. Large-scale semi-arid afforestation can enhance precipitation and carbon sequestration potential. Sci. Rep. 8 (1), 996.
Zhang, M., Wei, X., 2021. Deforestation, forestation, and water supply. Science 371 (6533), 990–991.
Zhi, C., Cai, Z., Liu, X., Li, X., 2018. Spatial-Temporal Analysis of Cooling Effect of Urban Water Bodies in Chongqing, China. Remote Sens 10, 702.
Zhou, L., Chen, H., Dai, Y., 2015. Stronger warming amplification over drier ecoregions observed since 1979. Environ. Res. Lett. 10 (6), 064012.
Zhou, W., Huang, G., Cadenasso, M.L., 2014. Does spatial configuration matter? Understanding the effects of land cover pattern on land surface temperature in urban landscapes. Landsc. Urban Plan. 102 (1), 54–63.

Further reading

Gao, B., Yang, J., Chen, Z., Sugihara, G., Li, M., Stein, A., Wang, J., 2023. Causal inference from cross-sectional earth system data with geographical convergent cross mapping. Nat. Commun. 14 (1), 5875.
Kumar, M., Denis, D.M., Singh, S.K., Szabó, S., Suryavanshi, S., 2018. Landscape metrics for assessment of land cover change and fragmentation of a heterogeneous watershed. Remote Sens. Appl.: Soc. Environ. 10, 224–233.
Sugihara, G., May, R., Ye, H., Hsieh, C.H., Deyle, E., Fogarty, M., Munch, S., 2012. Detecting causality in complex ecosystems. science 338 (6106), 496–500.